Linking the kinetic energy fraction and equivalent length method for trickle irrigation design under local losses

Giorgio Baiamonte, M.ASCE

Department of Agricultural, Food and Forest Sciences (SAAF), University of Palermo, viale delle Scienze, Building 4, 90128 Palermo, ITALY.

Abstract

New methods using analytical relationships to design drip irrigation laterals and subunits have been introduced in recent years based on the assumption that minor losses can be neglected. This assumption could be relaxed by applying the equivalent method, which makes it possible to account for minor losses, such as those caused by emitter connections, through formulae based on the rationale that an equivalent length of the drip lateral produces the same losses. However, equivalent length formulas are empirical, thus, they do not necessarily cover the entire range of conditions in the real-world contexts where the same formulas will be applied and their extrapolation could lead to erroneous results.

In this paper, theoretical equivalent lengths are calculated and linked to the kinetic energy fraction, which is considered an alternative general procedure to compute minor losses. Therefore, the results obtained here are valid in all general contexts, since they are not affected by experimental calibrations. A methodology is suggested that extends the use of analytical relationships to design drip laterals from a previous method that neglects minor losses, to a new method in which minor losses are considered. Several applications are performed for drip laterals in horizontal as well as in sloping fields. Results show the reliability of this new design procedure.

Key-Words: drip irrigation, minor losses, equivalent length, kinetic energy fraction

Introduction

Some simple relationships used to design drip laterals have been introduced during the past few years (Valiantzas 1998; Baiamonte et al. 2015; Baiamonte 2018c). More recently, these relationships have been extended to trickle irrigation subunits (Baiamonte 2018e). In particular, by neglecting emitter flow rate variations and the local losses along the lateral, Baiamonte et al. (2018e) suggested an analytical approach to optimally design micro-irrigation subunits applicable to any lateral and manifold slope and developed the software IRRILAB (IRRILAB, 2018) to facilitates their design. This analytical procedure, like others introduced in different contexts (Baiamonte 2016d; Baiamonte and Singh 2016a; 2016b; Broadbridge et al., 2017), makes it easy to understand the factors affecting the microirrigation unit design. Moreover, it also provides the optimal pressure head and emitter flow rate, i.e., the coefficient k_e of the emitter flow rate-pressure head relationship, which minimize the energy consumptions.

By maintaining the hypothesis of negligible minor losses, Baiamonte (2016a) detected the exact best manifold position (*BMP* = 0.24, under the Blasius resistance equation) for any lateral slope, which must be fixed for an optimal design. Specifically, this *BMP* value makes it possible to reach the maximum allowable emitter pressure at the inlet and at the distal end of a downhill lateral, and the minimum allowable pressure at the distal end of an uphill lateral and upstream of the distal end in a downhill lateral. Moreover, it was found that the *BMP*, which allows the use of the entire imposed pressure range variability, corresponds to the only manifold position where it is possible to minimize the required energy. Slightly different *BMP* values were found using two different resistance formulas, *BMP* = 0.25 and 0.26, for the Hazen-Williams and Darcy-Weisbach equations, respectively (Baiamonte 2018b), which were considered in IRRILAB.

It should be noted that the ‘optimal’ design introduced above only refers to an ‘optimal’ distribution of the emitter pressure head along the laterals that minimizes the energy required, and it does not lead to the minimum annual cost including investment cost, since no economic analysis associated with the above procedures was carried out. This aspect was addressed by Carrión el al. (2013), who developed a software application named PRESUD that made it possible to identify the optimum micro-irrigation subunit using the annual water application cost per unit of irrigated area. Wang et al. (2015) also presented an economic optimization method that seeks to balance competing costs and benefits and, Jiménez-Bello et al. (2015) and Fernández García et al. (2015) also dealt with the same issue at the wider scale of pressurized irrigation systems (rather than subunits). More recently, Chamba et al. (2019) introduced a novel approach where the diameters of the laterals and submains were calculated by minimizing an objective cost function that includes investment and operating costs of drip irrigation units and minor losses were considered according to the equivalent length method.

Although, the procedures proposed by Baiamonte et al. (2015) and Baiamonte (2018c; 2018e) are analytical and do not require recursive and finite element techniques in contrast to other design methodologies (Wu et al. 1983; Gill et al. 1989; Al-Amoud 1995; Wu 1997; Kang and Nishiyama 1996; Kang et al.1996; Kang 2000), or design charts (Wu and Gitlin 1975), they neglect minor losses due to emitter insertions in the lateral. Thus, they can only be applied when the emitter connections do not significantly reduce the lateral cross section. However, although each individual emitter usually only determines a slight local head loss (at insertion point), the sum of all local losses in a lateral can become significant, especially when emitter spacing is very small resulting in many emitters to be inserted along a drip lateral (Howell and Barinas 1980; Al-Amoud 1995, Juana et al. 2002a; Yıldırım 2007; Rettore Neto 2009). In fact, many studies have recognized the need to account for minor losses and the dependence of minor losses on the geometry of the emitters (Howell and Barinas 1980; Provenzano and Pumo 2004; Palau-Salvador et al. 2006).

Palau-Salvador et al. (2006) proposed a procedure for calculating the local losses of on-line emitters that depends on the number of emitters, the average emitter flow rate, and the ratio between the area of the emitter’s protrusion and the cross-sectional area of the pipe. For on-line emitters, Rettore Neto et al. (2009) suggested a new method to estimate minor head losses within the emitters, considering the obstruction determined by the insertion of the emitters and proposed an equation to simplify the calculation of an emitter's minor loss.

Yildirim (2010) proposed a simplified mathematical model based on the backward stepwise procedure which incorporates simple theoretical expressions for three energy loss components (local and friction losses due to emitters and pipe friction losses) to finally evaluate total energy losses along a trickle lateral line with integrated in-line and/or on-line emitters. Zitterel et al. (2014) used Buckingham's theorem in a method to detect the variables affecting minor losses in the lateral due to the flow passage of the emitter connectors. Juana et al. (2002a) suggested a procedure to analyze minor losses at emitter insertions that is based on principles of fluid mechanics, which support Bélanger's expression, thus allowing more rational, vs. completely empirical, predictions than those offered by other approaches.

Minor losses may be considered by applying the equivalent method (Watters and Keller 1978; Chamba et al. 2019), which makes it possible to account for minor losses in terms of the equivalent length, *EL*, of the drip lateral producing the same minor losses. For example, Watters et al. (1977) introduced a table of equivalent lateral lengths to qualitatively estimate the size of the barb. Pitts et al. (1986) used Watters and Keller's (1978) data, who derived an equivalent length relationship as a function of the lateral inside diameter, D (Table 1), to propose a new one based on the barb diameter, D_b (for $3.8 \leq D_b \leq 7.6$ mm) and lateral diameter, D (Table 1). These relationships could help account for minor losses when applying the aforementioned analytical solutions. However, the previously mentioned equivalent length formulae are empirical, thus they do not necessarily cover the entire range of conditions in which the same formulae may be applied, and consequently, their extrapolation could lead to erroneous results. As an example, Juana et al. (2002b) found a larger dispersion of *LE* values when lateral head losses were small and that the inlet head, Reynolds number, and emitter spacing did not show a clear effect on *LE* values.

As an alternative to the equivalent method, minor losses can also be expressed in the classic and more general form, as a fraction of the kinetic load, α_L, obtained by the Reynolds similarity principle, where the minor losses coefficient, α_L, depends on the geometric characteristics of the emitter insertion point and the Reynolds number (Rettore Neto et al. 2009). However, the latter procedure complicates the derivation of the aforementioned analytical relationships for the design of micro-irrigation systems and until now has been poorly attempted. For integrated laterals, in which coextruded emitters are installed inside the pipe, Provenzano and Pumo (2006) presented a power relationship between the coefficient, α_L, expressing the amount of local losses as a fraction of the kinetic head, and a simple geometric parameter characterizing the geometry of the emitter and the pipe (Table 1). Provenzano and Pumo (2006) also compared their relationship with that previously calibrated for on-line emitters (Bagarello et al. 1997), as a function of the pipe-emitter geometry, by using experimental measurements (Table 1).

In conclusion, this feature is widely discussed and a general methodology to estimate minor losses according to the equivalent method, which does not depend on self-calibration, has not yet been found.

In this paper, first the relationship between the equivalent length and the minor losses coefficient is theoretically derived and illustrated by varying the important design variables influencing minor losses, i.e., the emitter flow rate, the inside pipe diameter, and the emitter spacing.

Second, a methodology suggesting how to extend the analytical relationships to design both horizontal and sloped drip laterals is introduced, extending a previous procedure that was derived by neglecting minor losses (Baiamonte 2018c) to one in which minor losses are considered.

Third, once this procedure has been derived, one of the objectives of this work is to also show some applications of the extended procedure, when the coefficient k_e and the exponent x of the emitter flow rate-pressure head relationship are imposed as equal to the commercial specifications. Moreover, the emission uniformity coefficient, EU, was linked to the pressure head tolerance, for any emitter's characteristics, facilitating the drip lateral design.

Horizontal drip laterals

For an uphill drip lateral, by imposing the maximum pressure, h_{max}, at the inlet, and the minimum pressure, h_{min}, at the distal end of the uphill lateral, and by considering minor losses, Baiamonte (2018d) reported the following energy balance equation:

$$2\,\delta\, h_{*n} + n_u S_0 - H_{n_u}^{(-r)} K - \left(\frac{n_u^2}{3} + \frac{n_u}{2} + \frac{1}{6}\right) n_u\, \alpha_L\, K_{*L} = 0 \qquad (1)$$

where δ is the pressure head tolerance, h_{*n} denotes the average (design) emitter pressure head, h_n [m], normalized with respect to the emitter spacing, S [m], r is the flow rate exponent of the flow resistance formula, n_u is the number of the emitters in the uphill lateral, $H_{n_u}^{(-r)}$ is the corresponding generalized harmonic number of order -r, truncated at n_u equal to $H_{n_u}^{(-r)} = \sum_{k=1}^{n_u} 1/k^r \;\; /; n_u \in N$.

In Eq. (1), K is a parameter that accounts for friction losses (friction head loss gradient) that according to the Blasius's resistance equations, is commonly used for smooth-walled polyethylene pipe (Keller and Bliesner 1990), and can be expressed according to the monomial power-law:

$$K = \frac{0.316 \cdot 2^2 \sqrt{2}}{g\, \pi^r}\, \nu^{0.25}\, \frac{q_n^r}{D^s} \qquad (2)$$

in which q_n [m^3 s^{-1}] is the average (design) emitter discharge, D [m] is the inside pipe diameter, g [m s^{-2}] is the acceleration of gravity, ν = 1.008 10^{-6} m^2 s^{-1} is the water's kinematic viscosity at the standard 20 °C water temperature. For the Blasius's resistance equations considered here, r and s are equal to 1.75 and 4.75, respectively.

Minor losses in Eq. (1) are expressed by $\alpha_L K_{*L}$ (De Marchi 1954), i.e., the minor loss coefficient α_L multiplied by the kinetic energy, K_L, associated with q_n, and normalized with respect to the emitter spacing, S. Thus, for a design emitter flow rate, q_n, flowing in the lateral, $\alpha_L K_{*L}$ can be expressed according to the monomial power-law:

$$\alpha_L K_{*L} = \frac{\alpha\, 8\, q_n^2}{g\, \pi^2 D^4 S} \tag{3}$$

For $\alpha_L = 0$ the minor loss is zero and for $\alpha_L = 1$, the minor loss is equal to the dynamic pressure head. The minor loss coefficient can also be greater than the unity for some components in the hydraulic design, however, this occurrence is seldom achieved for drip laterals where α_L usually is in the 0-0.7 range (Juana et al. 2002a; Yıldırım 2007).

Eq. (1) and Eq. (2) show that, for a fixed pressure head tolerance, δ, the mathematical formulation of the law of conservation of energy is satisfied, so that the pressure head variation (first term) is balanced by potential energies (second term), friction (third term) and minor losses (fourth term) variations.

For horizontal laterals, the energy balance equation can be rewritten following Eq. (1), by relaxing the slope term and by replacing the number of emitters of the uphill lateral n_u with $n_{d,L}$, which denotes the number of the emitters when minor losses are considered:

$$2\delta h_{*n} - H_{n_{d,L}}^{(-r)} K - \left(\frac{n_{d,L}^3}{3} + \frac{n_{d,L}^2}{2} + \frac{n_{d,L}}{6} \right) \alpha_L K_{*L} = 0 \tag{4}$$

Therefore, when minor losses are considered, emitter spacing that is normally related to agronomics and infiltration characteristics of soils (Baiamonte, 2020) is a scale factor of two terms in the energy balance equation.

Linking the minor loss coefficient α_L, i.e., the kinetic energy fraction accounting for minor losses, to the equivalent length, requires denoting *EL* as the fraction of emitters (or of the lateral length, L_d) when minor losses are neglected, n_d, which are needed for the same minor losses:

$$EL = \frac{n_d - n_{d,L}}{n_d} = \frac{L_d - L_{d,L}}{L_d} \tag{5}$$

where *EL* is the equivalent length fraction, L_d is the lateral length when minor losses are neglected and $L_{d,L}$ is the lateral length when minor losses are considered, which for any *S* are associated with n_d and $n_{d,L}$, respectively. Note that $L_d - L_{d,L}$ is the most common equivalent length expression, l_e, which is usually used to account for minor losses (Juana et al., 2002a) by multiplying friction losses by $(1 + l_e/S) = (1 + (n_d - n_{d,L}))$, thus Eq. (5) could be used to determine l_e, accordingly.

Of course, if *EL* is known, Eq. (5) allows the determination of the number of emitters (and therefore lateral length) when accounting for minor losses, $n_{d,L}$:

$$n_{d,L} = n_d\left(1 - EL\right) \tag{6}$$

and the corresponding lateral length, $L_{d,L} = n_{d,L}\, S$. For horizontal laterals, n_d can be determined for any design parameter by using the solution reported in Baiamonte (2018c, 2018e), which is valid when minor losses are neglected, as observed above:

$$n_d = 25\,\frac{\delta^{1/(1+r)} h_{*n}^{1/(1+r)}\, D^{s/(1+r)}}{q_n^{r/(1+r)}} = 1.85\left(\frac{\delta\, h_{*n}}{K}\right)^{1/(1+r)} \tag{7}$$

Indeed, for horizontal laterals, the design problem can be solved by just using Eq. (7) and considering the emitters' flow rate–pressure head relationship:

$$h_n = \left(\frac{q_n}{k_e} \right)^{1/x} \tag{8}$$

where k_e and x are the coefficient and the exponent of the emitters' flow rate–pressure head relationship. Therefore, the design problem only requires EL when minor losses are considered.

Before determining an explicit EL solution for any α_L value, it is interesting to study the relationship between EL and the minor losses coefficient, α_L, in dimensional terms by varying the important design variables influencing minor losses, i.e., q_n, D, and the emitter spacing, S. Towards this aim, substituting Eq. (3), Eq. (4), Eq. (6) and Eq. (8) in Eq. (2) gives the following implicit EL relationship:

$$\alpha_L = \frac{3\pi^{0.25} D^4}{2\, n_d \,(1-EL) q_n^2} \frac{\delta\, q_n^{1/x}\, k_e^{-1/x}\; g\, \pi^r - 0.316 \cdot 2\sqrt{2}\, \nu^{0.25} q_n^r\, D^{-s} S\, H_{n_d\,(1-EL)}^{(-r)}}{(1+n_d\,(1-EL))(1+2n_d\,(1-EL))} \tag{9}$$

making it possible to plot the $EL(\alpha_L)$ relationship for any δ, D, q_n, S, k_e and x. The EL vs. α_L coefficient was graphed by assuming the common pressure head tolerance $\delta = 0.1$ (Singh et al. 2015) and the drip lateral characteristics reported in Table 2 (#2), which pertains to TANDEM and JUNIOR® drip laterals, made by IRRITEC.

Fig. 1 shows the relationships between the equivalent length, EL, and the minor losses coefficient, α_L, for different emitter spacing, S, corresponding to a fixed D = 13.6 mm and for different q_n values (Fig. 1a) and to a fixed q_n = 2.1 l/h for different D values (Fig. 1b). Eq. (8) verifies that an average emitter pressure $h_n = (2\, q_n\, k_e^{-1}\, ((1+\delta)^x + (1-\delta))^{-1})^{1/x}$ corresponds to a fixed pressure head tolerance, δ, for any average q_n. As expected, EL is zero for $\alpha_L = 0$, and then increases with α_L. For fixed α_L and D, EL increases with increasing q_n and with decreasing S (Fig. 1a) and, for fixed α_L and q_n, EL increases with increasing D and with decreasing S (Fig. 1b). This D effect differs from what might be expected (smaller minor losses expected with larger D), however it is not surprising if we consider that, when designing drip laterals according to the suggested criterion (h_{max} = (1+δ) h_n and h_{min} = (1- δ) h_n), for fixed q_n, with increasing D, n_d also increases with fixes S, which in turn causes local losses and equivalent lengths to increase. According to Keller and Karmeli (1974), δ = 0.1 implies a known emission uniformity coefficient, EU for horizontal laterals, depending on x, which will be discussed later. An application was performed for α_L = 0.4, i.e. by assuming EL = 0.194 (Fig. 1).

Fig. 2 illustrates the pressure head lines derived by applying the SBS procedure a) for α_L = 0 and b) for α_L = 0.4, and by assuming L_d = 50 m (Eq. 7, for α_L = 0) and $L_{d,L}$ = 50 (1 - 0.194) = 40.3 m (Eq. 6, for α_L = 0.4 and EL = 0.194).

The numerical SBS procedure was applied to test the consistence of the results obtained by the suggested procedure (Sadeghi et al., 2015), allowing the verification of Eq. (9). In particular, if minor losses are neglected (α_L = 0) in the lateral design (Eq. 7), the SBS procedure provides the optimal drip lateral, whereas α_L = 0.4 results in a design in which the pressure head falls below the allowable range (Fig. 2a). On the contrary, if minor losses are considered in the lateral design (for α_L = 0.4, EL = 0.194), the SBS procedure for α_L = 0.4 provides the optimal drip lateral, whereas α_L = 0, provides an overestimation of pressure heads (Fig. 2b).

Although Eq. (9) gives results that are exact and consistent to what is expected, it can't be easily applied for practical applications, for which a α_L value is assumed and the unknown equivalent length EL needs to be determined. In order to overcome this issue, Eq. (2) may be rearranged as a function of three groups of variables, $\alpha_L K_{*L}/K$, $\delta h_{*n}/K$ and n_d, thereby allowing the number of design variables to be reduced:

$$\alpha_L \frac{K_{*L}}{K} = \frac{6\left(2\,\delta\,\frac{h_{*n}}{K} - H^{(-r)}_{n_d(1-EL)}\right)}{2\left(n_d\,(1-EL)\right)^3 + 3\left(n_d\,(1-EL)\right)^2 + \left(n_d\,(1-EL)\right)} \qquad (10)$$

For fixed n_d values, i.e., for fixed $\delta h_{*n}/K$ (see Eq. 7), Eq. (10) was solved for EL values rounded to one decimal place, and the corresponding $\alpha_L K_{*L}/K$ parameters are reported in Table 3, which can be used for practical purposes.

As an example, for the application illustrated in Fig. 2 ($n_d = L_d/S = 250$), it can be verified that $\alpha_L K_{*L}/K$ equals 0.233, which is close to the tabular value ($\alpha_L K_{*L}/K = 0.245$), for which the corresponding EL equals 0.2, which is close to $EL = 0.194$, as assumed above.

In order to implement the proposed procedure in the IRRILAB software application (Baiamonte, 2018e), where minor losses are neglected, an EL calculus was extended to any fixed EL value following an approximated procedure. It should be noted that the latter is required for application purposes, for which EL rather than α_L, is the calculated variable, whereas Eq. (10) provides α_L for any EL, according to an exact analytical solution. To make Eq. (10) explicit in EL, the range of the group's $\delta h_{*n}/K$ and $\alpha_L K_{*L}/K$ parameters was considered according to Table 4, covering a wide combination of different design variables.

For different n_d values, Fig. 3 illustrates an interesting shape of the relationship between EL and $\alpha_L K_{*L}/K$, suggesting that these relationships could overlap if $\alpha_L K_{*L}/K$-shifted along the log axis. If we use the $\alpha_L K_{*L}/K$ values for a high $n_d = 10000$, $(\alpha_L K_{*L}/K)_{10000}$, as a reference variable, the latter can be determined for any $\alpha_L K_{*L}/K$, by shifting $\mathrm{Log}(\alpha_L K_{*L}/K)$ according to:

$$\left(\frac{\alpha_L K_{*L}}{K}\right)_{10000} = 10^{c_H + Log\left(\alpha_L K_{*L}/K\right)} \tag{11}$$

where, for each n_d value, the c_H constant was determined by minimizing the standard error of the estimate, SEE. Fig. 4a plots the relationship between EL and $\alpha_L K_{*L}/K$, shifted according to Eq. (11), for different n_d, indicating that the overlap is fine for low EL values and a bit worse for $EL > 0.8$. However, by imposing a minimum $n_d = 15$, the overlapping is fine in the entire EL domain as shown in Fig. 4b. The latter $n_d > 15$ assumption, which is common in practice, was also imposed in Baiamonte (2018c, 2018e) when deriving simple design relationships for the laterals as well for the manifold, in order to provide very moderate errors in the design of the laterals and of the manifold (<2.5%).

A simple linear regression between Log(n_d) and the c_H constant was performed ($R^2 = 1$) in order to the derive the following relationship, which is necessary for the approximated design procedure:

$$c_H = 0.244\, Log(n_d) - 0.978 \qquad (12)$$

Eq. (12) is plotted in Fig. 5a, together with the c_H values obtained by minimizing the standard error of the estimate, SEE.

Overlapping of the shifted $EL(\alpha_L K_{*L}/K)$ curves for any n_d, allows detecting an approximated EL-$\alpha_L K_{*L}/K$ relationship by just considering the relationship for the reference variable $EL(\alpha_L K_{*L}/K)_{10000}$. A fitting of the EL vs. the $(\alpha_L K_{*L}/K)_{10000}$ parameter to the derived EL function was attempted by selecting the 3-parameter Fréchet distribution, also known as the inverse Weibull distribution, which is a special case of the generalized extreme value distribution. The Fréchet EV2 was also used by Baiamonte (2017) to describe the best manifold position for drip laterals on concave and convex slopes. The cumulative distribution function (Fréchet EV2, CDF) of the generalized form that includes a location parameter μ, and a scale parameter $\sigma > 0$, is written here:

$$EL = exp\left(-\left(\frac{\sigma}{\left(\frac{\alpha_L K_{*L}}{K}\right)_{10000} - \mu}\right)^{\gamma}\right) \quad \text{for} \quad \left(\frac{\alpha_L K_{*L}}{K}\right)_{10000} > \mu \qquad (13)$$

where $\gamma > 0$ is a shape parameter. In the case $\mu = 0$ Eq. (13) can be written as:

$$EL = exp\left(-\left(\frac{\sigma K_{10000}}{\alpha K_{*L,10000}}\right)^{\gamma}\right) \tag{14}$$

By minimizing the standard error of the estimate, SEE, between theoretical and fitted EL values, the parameters γ, σ and μ reported in Table 5 were obtained. Table 5 also reports the γ and σ parameters calculated in the case $\mu = 0$ (Eq. 14), which of course corresponds to a slightly greater SEE than when $\mu > 0$ is assumed (Table 5).

As can be observed in Eq. (13) and Eq. (14), the Fréchet CDF satisfies the limiting condition, $EL \sim 1$, for $\alpha_L \sim \infty$. Whereas for $EL \sim 0$, only Eq. (14) gives the expected condition $\alpha_L = 0$. However, Eq. (13) corresponds to a lower SEE and for this reason will be considered in the following.

For different n_d, Fig. 4b plots Eq. (13), showing a good fit of the exact $EL(\alpha_L K_{*L}/K)_{10000}$ relationship. Thus, Eq. (13) can be used to determine the EL value for a fixed $(\alpha_L K_{*L}/K)_{10000}$. In conclusion, for an assigned n_d value, Eq. (11) and Eq. (12) allow the determination of $(\alpha_L K_{*L}/K)_{10000}$ and c_H, whereas an assigned $\alpha_L K_{*L}/K$, Eq. (13) allows EL to be calculated.

As an example, for the application illustrated in Fig. 2, for which $n_d = 250$ (Eq. 7) and $\alpha_L K_{*L}/K = 0.234$ (Eq. 4 and Eq. 1), Eq. (12) and Eq. (11) give $c_H = -0.374$ and $(\alpha_L K_{*L}/K)_{10000} = 0.099$, respectively. For the latter, Eq. (13) with the parameters reported in Table 5, gives $EL = 0.207$, which is close to the exact EL previously calculated and also to the tabular EL.

The reliability of the suggested procedure to determine the EL was verified for any n_d and $\alpha_L K_{*ML}/S_0$ values. For the same n_d values (with $n_{d,ML} = n_d$ (1-EL) > 15) and $\alpha_L K_{*ML}/S_0$ ranges considered in Fig. 4b (Table 4), covering most of the practical cases, Fig. 5b compares the exact EL values with those calculated by using Eq. (13), with the $(\alpha_L K_{*L}/K)_{10000}$ values and c_H values calculated by using Eq. (11) and Eq. (12), respectively. The comparison showed a good agreement between exact and approximated EL values (SEE = 0.0051, N = 798).

The median of the Fréchet CDF makes it possible to detect the $EL(\alpha_L K_{*L}/K)_{10000}$ value corresponding to EL = 0.5, $(\alpha_L K_{*L}/K)_{10000}^{\text{median}}$, and has the following expression:

$$\left(\frac{\alpha_L K_{*L}}{K}\right)_{10000}^{\text{median}} = \mu + \frac{\sigma}{\sqrt[\gamma]{log\,2}} \qquad (15)$$

Eq. (15) gives $(\alpha_L K_{*L}/K)_{10000}^{\text{median}}$ = 0.7687 and could allow the calculation of the median of the $EL(\alpha_L K_{*L}/K)$ function, $(\alpha_L K_{*L}/K)^{\text{median}}$, i.e. for any n_d value, by inverting Eq. (12) and by using Eq. (15):

$$\left(\frac{\alpha_L K_{*L}}{K}\right)^{median} = 7.307\, n_d^{-0.244} \qquad (16)$$

Eq. (16) is tested in Fig. 3 where $(\alpha_L K_{*L}/K)^{\text{median}}$ values calculated by Eq. (16) are plotted (cross symbols).

Sloped drip laterals

For paired sloped drip laterals, Baiamonte (2018d) showed that the best manifold position, BMP = 0.24, which was derived under the Blasius resistance equation and by neglecting minor losses Baiamonte (2018c), could also be used when minor losses are considered. Therefore, the energy balance equation for the uphill-sloped lateral need not be considered and the simple optimal downhill lateral design (BMP = 0), is only governed by three equations rather than four (Baiamonte 2018d).In the following they are rewritten for any EL as a function of the groups of variables $\alpha_L K_{*L}/S_0$, $\delta h_{*n}/S_0$, and as a function of n_d and i_{min}:

$$\left(H^{(1-r)}_{n_d(1-EL)-i_{min}} - \zeta(1-r)\right) r \frac{K}{S_0} - 1 + \left(\left(n_d(1-EL) - i_{min}\right)^2 + \left(n_d(1-EL) - i_{min}\right) + \frac{1}{6}\right)\alpha_L \frac{K_{*L}}{S_0} = 0 \qquad (17)$$

$$2\,\delta \frac{h_{*n}}{S_0} + i_{min} - \left(H^{(-r)}_{n_d(1-EL)} - H^{(-r)}_{n_d(1-EL)-i_{min}}\right)\frac{K}{S_0} - \left(\frac{1}{6}(i_{min}-1)(2\,i_{min}-1) - n_d(1-EL)\left((i_{min}-1) - n_d(1-EL)\right)\right) i_{min}\,\alpha_L \frac{K_{*L}}{S_0} = 0 \qquad (18)$$

$$n_d(1-EL) - H^{(-r)}_{n_d(1-EL)}\frac{K}{S_0} - \left(\frac{\left(n_d(1-EL)\right)^3}{3} + \frac{\left(n_d(1-EL)\right)^2}{2} + \frac{n_d(1-EL)}{6}\right)\alpha_L \frac{K_{*L}}{S_0} = 0 \qquad (19)$$

where i_{min} is the emitter at the downhill lateral for which the minimum value of the pressure head occurs, counted from the inlet at the top of the lateral. Note that Eq. (22a) reported in Baiamonte (2018c), linking $\delta h_{*n}/S_0$ and n_d when minor losses are neglected, can be applied when minor losses are considered according to the equivalent method, i.e. by replacing n_d with n_d (1-EL):

$$\delta \frac{h_{*n}}{S_0} = \frac{n_d(1-EL)}{5.58} \qquad (20)$$

For the sake of simplicity, since uphill laterals are not taken into account, the lateral slope in Eqs. (17, 18, 19 and 20) is assumed to be positive for downhill laterals, rather than negative, as in Baiamonte (2018d). Note that in the same Eqs. (17, 18, 19 and 20), with respect to horizontal laterals (Eq. 10), the i_{min} parameter must be considered, and as well as the fact that $\alpha_L K_{*L}$ and δh_{*n} is divided by S_0, rather than by K as for horizontal laterals (Eq. 10).

Eq. (17), Eq. (18) and Eq. (19) make it possible to plot the relationships between the involved dimensionless groups, as illustrated in Fig. 6. In particular, by varying n_d, Fig. 6a, Fig. 6b and Fig. 6c show EL vs. $\alpha_L K_{*L}/S_0$, EL vs. $\delta h_{*n}/S_0$, and EL vs. i_{min} relationships, respectively. For each n_d value, in

Fig. 6b the pairs (EL, $\delta h_{*n}/S_0$) obtained by using Eq. (20) are also reported (cross symbols), validating the design relationship for sloped laterals, introduced in Baiamonte (2018c).

A good approximation of the i_{min} relationship can also be obtained if one observes that the curves plotted in Fig. 6c can be scaled with respect to those reported in Fig. 6b. The following relationship was derived:

$$i_{min} = 2.438\,\frac{\delta h_{*n}}{S_0} = 0.436\; n_d\,(1 - EL) \qquad (21)$$

which, according to Eq. (20) was also written as a function of n_d. In the right hand term of Eq. (21), the influence of the lateral slope, S_0, on i_{min} is not explicitly seen, but rather implied by the optimal number of the emitters, n_d, which in turn depends on S_0. Eq. (21) could be used in practice once n_d and EL are known, for controlling the most low-pressure sensitive emitter in the downhill lateral where the minimum pressure head, i_{min}, occurs.

It is interesting to observe in Fig. 6a that $EL(\alpha_L K_{*L}/S_0)$ relationships have the same shape of those corresponding to horizontal laterals (Fig. 3). Similarly to the reliability test of Eq. (20), cross symbols in Fig. 6c refer to the approximated i_{min} values calculated by Eq. (21), indicating that the same relationship also produce results that are a good approximation of the exact ones obtained by solving the system of Eqs. (17-19).

Analogously to horizontal laterals, the relationships illustrated in Fig. 6a could overlap if $\alpha_L K_{*L}/S_0$-shifted along the log axis. By once again assuming the $\alpha_L K_{*L}/S_0$ variable for n_d = 10000, $(\alpha_L K_{*L}/S_0)_{10000}$, as a reference variable, the latter can be determined for any $\alpha_L K_{*L}/S_0$, by shifting according to:

$$\left(\frac{\alpha_L K_{*L}}{S_0}\right)_{10000} = 10^{\,c_s + Log(\alpha_L K_{*L}/S_0)} \qquad (22)$$

where for each n_d value, the c_S constant was determined by minimizing the standard error of the estimate, SEE. Fig. 7a plots the relationship between *EL* and $\alpha_L K_{*L}/S_0$, shifted according to Eq. (22), for different n_d, indicating that the overlap is fine for low *EL* values and gets a bit worse for *EL* > 0.8, as it does for horizontal laterals (Fig. 4a). However, by once again imposing a constraint of n_d values greater than 15, the overlapping is fine in the entire *EL* domain, as shown in Fig. 7b.

Similarly to the case of horizontal laterals (Fig. 5), in order to derive an approximated design relationship explicit in *EL*, a simple linear regression was performed between Log(n_d) and the c_S constant:

$$c_S = 1.984\, Log(n_d) - 7.947 \qquad (23)$$

A comparison between c_S values obtained by minimizing the standard error of the estimate, SEE, and Eq. (23) is plotted in Fig. 8a (R^2 = 1). A fitting of the *EL* vs. $(\alpha_L K_{*L}/K)_{10000}$ was attempted by selecting the 3-parameter Fréchet distribution:

$$EL = exp\left(-\left(\frac{\sigma}{\left(\frac{\alpha_L K_{*L}}{S_0}\right)_{10000} - \mu}\right)^{\gamma}\right) \qquad (24)$$

where γ, σ and μ parameters were obtained by minimizing the standard error of the estimate, SEE, again between the theoretical and the fitted *EL* values, reported in Table 5. Contrarily to horizontal laterals, it was found that the 2-parameter Fréchet distribution did not show a good fit, therefore only the 3-parameters Fréchet distribution was considered. For the γ, σ and μ parameters reported in Table

5, Eq. (24) is plotted in Fig. 7b, showing a good fit (Table 5) and thus confirming that Eq. (24) can be used to determine EL for any n_d and $\alpha_L K_{*L}/S_0$ values.

Again, for $n_{d,L} = n_d\,(1-EL) > 15$ and for $\alpha_L K_{*ML}/S_0$ ranges (Table 4) considered in Fig. 7b, covering most of the practical cases (Table 4), Fig. 8b compares the exact EL values with those calculated by using Eq. (24), with $(\alpha_L K_{*L}/S_0)_{10000}$ and c_S values calculated by Eq. (22) and Eq. (23), respectively. The comparison showed a good agreement between exact and approximated EL values (SEE = 0.0049, N = 1533).

Analogously to horizontal laterals, the median of the $EL(\alpha_L K_{*L}/S_0)_{10000}$ function, $(\alpha_L K_{*L}/S_0)_{10000}^{median}$ was calculated as:

$$\left(\frac{\alpha_L K_{*L}}{S_0}\right)_{10000}^{median} = \mu + \frac{\sigma}{\sqrt[\gamma]{\log 2}} \qquad (25)$$

providing $(\alpha_L K_{*L}/S_0)_{10000}^{median} = 8.300\cdot 10^{-8}$, which allows the computation, for any n_d value, of the median of the $EL(\alpha_L K_{*L}/S_0)$ relationship, $(\alpha_L K_{*L}/S_0)^{median}$, by inverting Eq. (23):

$$\left(\frac{\alpha_L K_{*L}}{S_0}\right)^{median} = 7.345\, n_d^{-1.984} \qquad (26)$$

Eq. (26) is tested in Fig. 6a where $(\alpha_L K_{*L}/K)^{median}$ values calculated by Eq. (26) are plotted (cross symbols).

In conclusion, according to the procedure introduced here, for a given fraction of the kinetic load, α_L, the equivalent length accounting for minor losses can be calculated on a theoretical basis, thus it is not affected by experimental calibrations. This latter feature makes it possible to extend the use of analytical relationships used to design drip laterals presented in the literature, or the lateral lengths suggested by the manufacturers, which are derived by neglecting minor losses, to the case in which minor losses are considered. Moreover, no iterative methods are required. Thus, the suggested procedure is less time-consuming and less labor-intensive than other experimental alternatives and offers a practical solution that is not affected by experimental calibration for laterals actually being designed for use in irrigation subunits.

The emission uniformity coefficient, *EU*, for any δ and *x*

The approximated solutions explicit in *EL* derived for horizontal and sloped laterals make it possible to extend the design relationships derived in Baiamonte (2018d), that are valid when minor losses are neglected, to the case in which minor losses are considered.

From a practical point of view, when emitter characteristics are established, it is useful to show some applications of the extended procedure, when the k_e and x coefficient are imposed, since k_e and x are derived by the original formula, i.e., by using q_n and h_n analytical solutions ($k_e = q_n/h_n^{1/x}$), that cannot fit the commercial k_e value. Indeed, the latter is a limitation in the methodology introduced in Baiamonte (2018c).

Moreover, in the same paper, the emission uniformity coefficient, *EU*, linked to the pressure head tolerance, δ, for $x = 0.5$ (cf. Fig. 9b in Baiamonte 2018a), needs to be extended to any x value. Towards this aim, the same linear relationships linking the pressure head tolerance, δ, and *EU* (Keller and Karmeli 1974), introduced in Baiamonte (2018a), have been considered. Furthermore, these relationships, aside from $x = 0.5$, were derived by neglecting the manufacturing coefficient of variation, C_v, and for a number of emitters per plant, $n_p = 1$, according to different five lateral layouts. In this section, δ versus *EU* relationships will be extended to any C_v and n_p and x values.

The angular coefficient, m_{EU}, of δ versus *EU* linear relationships (cf. Fig. 9b in Baiamonte 2018a) can indeed be used to extend the formulation to any C_v and n_p. Accordingly, the linear *EU* versus δ relationship was modified as follows:

$$EU = \left(1 - \frac{\delta}{m_{EU}}\right)\left(1 - 1.27\, C_v\, n_p^{-0.5}\right) \qquad (27)$$

where m_{EU} is the angular coefficient, reported in Table 6, for different x values and for the layouts considered in Baiamonte (2018a) (downhill, horizontal and uphill), and for different values of the exponent x of the emitter q_n vs h_n relationship. The m_{EU} values were determined according to a desired scaling exponent, x, and following the same EU relationship of Keller and Karmeli (1974), as:

$$m_{EU} = \left(m_{EU,0.5}\right)^{2x} \qquad (28)$$

where $m_{EU,0.5}$ is the angular coefficient of δ versus EU relationships for x = 0.5. Of course, for x = 0.5, m_{EU} values reported in Table 6 match with those of Baiamonte (2018a, Fig. 9b). Values of m_{EU} that differ from those reported in Table 6 can also be calculated by using the fitting equations reported in Fig. 9, as a function of the exponent x of the emitters' flow rate–pressure head relationship, for downhill, uphill and horizontal drip laterals.

For x = 0.5, for downhill laterals (m_{EU} = 2.53) and for horizontal laterals (m_{EU} = 3.53), Eq. (27) is plotted in Fig. 10a and in Fig. 10b, respectively, with $C_v\, n_p^{-0.5}$ as a parameter. As will be shown later, knowledge of Eq. (27) and Eq. (28) makes it possible to calculate EU values for sloped and for horizontal drip laterals designed for any emitter (k_e, x) and for a fixed n_d. Of course, the average q_n, which is linked to h_n (Eq. 8) should not be confused with the mean flow rate that was considered in the Keller and Karmeli (1974)'s EU relationship.

In the next two sections, several applications were performed for drip laterals in horizontal as well in sloping fields, showing the reliability of the suggested new design procedure. The proposed procedure will be verified by applying an exact numerical step-by-step (SBS) procedure, with the additional aim of investigating the retained assumption from the aforementioned analytical solutions that the emitter flow rate variation along the lateral could be considered negligible (Baiamonte 2018c; 2018e).

Example applications for horizontal laterals

For horizontal laterals, let's assume that q_n is fixed and equal to the emitter flow rate reported in the manufacturer's catalogue, q_{cat} (Table 1 and Table 6), although any q_n value could be fixed depending on the many factors affecting soil permeability (Baiamonte et al. 2017). Assuming a pressure head tolerance $\delta = 0.1$, for which according to x value (Table 1) and to any C_v and n_p, EU could be calculated (Eq. 27). The number of emitters, n_d, is fixed and equal to that reported in Table 6 (second column).

Once D, q_n and are fixed, K can be calculated by using Eq. (3). Moreover, fixing S, n_d and δ makes it possible to calculate $\delta h_{*n}/K$, by inverting Eq. (7):

$$\frac{\delta h_{*n}}{K} = \left(\frac{n_d}{1.85}\right)^{1+r} \tag{29a}$$

which makes it possible to determine h_n:

$$h_n = S\frac{K}{\delta}\left(\frac{n_d}{1.85}\right)^{1+r} \tag{29b}$$

Then, calculate $\alpha_L K_{*L}/K$ (Eq. 4), c_H (Eq. 10) and $(\alpha_L K_{*L}/K)_{10000}$ (Eq. 11), which in turn allows EL to be determined (Eq. 13), thus $n_{d,L}$ (Eq. 6) and $L_{d,L} = n_{d,L}\, S$.

The above steps were followed to obtain the design parameters reported in Table 7, where C_v = 0 was assumed. The excessive h_n values, obtained for application #1 and #5, suggested that the n_d

value should be reduced, which allows a more feasible emitter pressure head, h_n, to be obtained, as reported in Table 7 (application #1bis and #5bis).

In order to test the consistence of the results reported in Table 7, Figure 11a plots the PHD lines by applying the SBS procedure. Results showed that PHD lines achieve the theoretical minimum pressure head h_n (1-δ), which are indicated by the dotted horizontal lines, as well as the theoretical maximum pressure head (1 + δ) h_n , which equals the inlet pressure head, h_{in}.

Applications were also performed by assuming the exponent x of the emitter reported in Table 2 in the SBS, in contrast with what was assumed in the suggested procedure, where the emitter flow variation was neglected. Fig. 11b showed that considering the emitter flow variation in the SBS procedure ($x > 0$) provides a slight upshift of the PHD lines, which is more evident as the lateral length increases. These results agree with Baiamonte (2018d, cf. Fig. 12 and Fig. 13), and confirm that, for fixed and appropriately low pressure head tolerances, neglecting flow variation in the approximate design procedure determines very moderate errors that are in the positive direction of increasing the minimum allowable pressure along the drip lateral. Indeed, even slightly higher pressure than the minimum, h_n (1 – δ), would favor the plants' wellbeing in lateral designs because an overestimation would not risk supplying less than the minimum water volume requirement.

Example applications for sloped laterals

For sloped laterals, combining Eq. (4a) and Eq. (4b) reported in Baiamonte (2018e) yields the emitter flow rate, q_n:

$$q_n = \frac{\alpha'}{\alpha} \frac{D^{s/r} S_0^{1/r}}{n_d} \tag{30}$$

where α = 0.1791 and α' = 19.028. Then, for a fixed α_L, calculate $\alpha_L K_{*L}/S_0$ and the corresponding reference value, $(\alpha_L K_{*L}/S_0)10000$, by using Eq. (4) and Eq. (22), respectively. The latter lets one calculate EL by Eq. (24), and $n_{d,L}$ by Eq. (6) and the corresponding $L_{d,L} = n_{d,L}\, S$.

For the selected parameters, a pressure head tolerance satisfying the characteristics of the emitters (k_e, x), δ_e, can be determined by combining Eq. (8), Eq. (20) and Eq. (30). An explicit δ_e relationship was derived:

$$\delta_e = \left(\frac{k_e}{\alpha'}\right)^{1/x} \frac{(\alpha\, n_d)^{1+1/x}\, S\,(1-EL)}{D^{s/r\,x}\, S_0^{1/r\,x-1}} \tag{31}$$

Once the modified δ_e, is known, the design emitter pressure head accounting for local losses, $h_{n,L}$ can be calculated by using Eq. (4b) reported in Baiamonte (2018c), after substituting δ_e to δ and $n_d = n_{d,L}$:

$$h_{n,L} = \alpha \frac{n_{d,L}\, S\, S_0}{\delta_e} \tag{32}$$

Of course, the inlet pressure head h_{in} can be calculated by using Eq. (31) and Eq. (32), i.e., $h_{in} = (1 + \delta_e)\, h_{n,L}$, whereas for $\delta = \delta_e$ and for any C_v and n_p, the corresponding EU can be calculated by Eq. (27).

Note that the adjustment of the emitter pressure head for sloped laterals is required (Eq. 32); whereas it was not needed for horizontal laterals, where the design problem is governed by just one condition.

For the same drip lateral characteristics considered for the horizontal case (Table 2), applications were also performed for sloped laterals, assuming that n_d is fixed and one wants to determine the EU (for $C_v = 0$). The corresponding results are reported in Table 8, whereas in Fig. 12, following the same application numbering reported in Table 8, the pressure distribution line and energy gradient lines are illustrated.

For case #4, the emitters' pressure head was too high ($h_{n,L}$ = 88.1 m), whereas the *EU* was too low for case #5 (with negative emitters' pressure heads, Fig. 12e), indicating that the emitter's characteristics and/or drip lateral diameter need to be changed and/or the lateral length needs to be decreased. For these two cases, the drip lateral was redesigned by reducing the drip lateral length (see #4bis and #5bis, in Table 8 and Fig. 12).

Table 9 illustrates the relative error (RE) of the maximum and minimum allowed pressure heads, of the i_{min}, and of the emission uniformity coefficient, *EU*, calculated by using the suggested procedure, with respect to those calculated according to the SBS procedure, for each application. Error analysis indicates that the suggested procedure is a good approximation of the exact one and thus, it could be used to extend the previous solutions and the IRRILAB software application, where minor losses were neglected, to the case in which minor losses are considered.

Summary

This paper extends recently introduced analytical relationships for designing drip irrigation laterals and subunits the case in which minor losses are relevant and need to be considered, i.e., when the morphology of emitter connections produces significant reductions of the lateral cross section.

Following the main finding, the most important results covered in this paper can be summarized as follows:

- For a given fraction of the kinetic energy (i.e. minor loss coefficient) accounting for minor losses, a theoretical methodology to derive the equivalent length, not affected by calibration is suggested.
- For horizontal laterals, the relationship between the equivalent length and the minor losses coefficient was studied by varying important design variables that influence minor losses (the emitter flow rate, the inside pipe diameter and the emitters' spacing).

- For horizontal laterals, the small influence of the retained hypothesis to neglect emitters' flow rate variations was shown.
- For both horizontal and sloped laterals, for a fixed emitter flow rate, inside pipe diameter, emitters' spacing, lateral length and slope, theoretically based relationships of the equivalent length fraction as a function of the kinetic energy fraction were proposed. Tabular equivalent length fractions and approximated relationships explicit in equivalent length were reported, which could be simple to use for practical purposes.
- For any emitter's characteristics (k_e and x), manufacturing variation coefficient and number of emitters per plant, a relationship between the emission uniformity coefficient, *EU*, of Keller and Karmeli (1974), and pressure head tolerance, δ, were suggested.
- Several applications were performed and tested by using the step-by-step procedure, for fixed emitter's characteristics (k_e and x) and for both horizontal and sloped laterals, showing the reliability of the extended formulas.

Data Availability Section

All data, models, and code generated or used during the study appear in the submitted article.

References

Al-Amoud, A.I. (1995). "Significance of energy losses due to emitter connections in trickle irrigation lines." *J. Agric. Eng. Res.*, 60(1), 1–5.

Bagarello, V., Ferro, V., Provenzano, G., and Pumo, D. (1997). "Evaluating pressure losses in drip-irrigation lines." *J Irrig Drain E-ASCE*, 123(1), 1–7.

Baiamonte, G. (2016a). “Simple Relationships for the Optimal Design of Paired Drip Laterals on Uniform Slopes.” *J Irrig Drain E-ASCE*, 142(2), 10.1061/(ASCE)IR.1943-4774.0000971, 04015054.

Baiamonte, G. (2016b). Closure to “Simple Relationships for the Optimal Design of Paired Drip Laterals on Uniform Slopes” by Giorgio Baiamonte, *J Irrig Drain E-ASCE*, 142(12), 10.1061/(ASCE)IR.1943-4774.0001126, 07016019.

Baiamonte, G. (2016c). Discussion of “Analysis of Geometrical Relationships and Friction Losses in Small-Diameter Lay-Flat Polyethylene Pipes” by Giuseppe Provenzano, Vincenzo Alagna, Dario Autovino, Juan Manzano Juarez, and Giovanni Rallo. *J Irrig Drain E-ASCE*, 142(10), 10.1061/(ASCE)IR.1943-4774.0001071, 07016013.

Baiamonte, G. (2016d). “Simplified model to predict runoff generation time for well-drained and vegetated soils.” *J Irrig Drain E-ASCE*, 142(11), 04016047, 10.1061/(ASCE)IR.1943-4774.0001072, 04016047.

Baiamonte, G. (2017). “Design of Concave and Convex Paired Sloped Drip Laterals.” *Agric. Water Manag.*, 191: 173-183, doi.org/10.1016/j.agwat.2017.06.015.

Baiamonte, G. (2018a). Erratum for “Simple Relationships for the Optimal Design of Paired Drip Laterals on Uniform Slopes.” *J Irrig Drain E-ASCE*, 144(2), 10.1061/(ASCE)IR.1943-4774.0000971, 08217003.

Baiamonte, G. (2018b). “Closed-form Solutions of Drip Laterals Balance Equation for Darcy-Weisbach Resistance Formula.” *J Irrig Drain E-ASCE*, 144(7), 04018011, 10.1061/(ASCE)IR.1943-4774.0001314.

Baiamonte, G. (2018c). “Advances in designing drip irrigation laterals.” *Agric. Water Manag.*, 199:157–174, https://doi.org/10.1016/j.agwat.2017.12.015.

Baiamonte, G. (2018d). “Minor Losses and Best Manifold Position in the Optimal Design of Paired Sloped Drip Laterals.” *Irrig. and Drain.*, https://doi.org/10.1002/ird.2274.

Baiamonte, G. (2018e). “Explicit Relationships for Optimal Designing of Rectangular Microirrigation Units on Uniform Slopes: the IRRILAB Software Application.” *Comput. Electron. Agr.*, 153:151-168, https://doi.org/10.1016/ j.compag.2018.08.005.

Baiamonte, G. (2020). “Analytical solution of the Richards equation under gravity-driven infiltration and constant rainfall intensity.” *J Hydrol E – ASCE*, 2020, doi: 10.1061/(ASCE)HE.1943-5584.0001933.

Baiamonte, G., Bagarello, V., D’Asaro, F., and Palmeri, V. (2017). “Factors influencing point measurement of near-surface saturated soil hydraulic conductivity in a small Sicilian basin.” *Land Degrad. Dev.*, 28, 970–982, doi:10.1002/ldr.2674.

Baiamonte, G., Provenzano, G., and Rallo, G. (2015). “Analytical Approach Determining the Optimal Length of Paired Drip Laterals in Uniformly Sloped Fields.” *J. Irrig. Drain E – ASCE.*, 141(1), 04014042, http://dx.doi.org/10.1061/(ASCE)IR.1943-4774.0000768.

Baiamonte, G., and Singh, V.P. (2016a). “Analytical solution of kinematic wave time of concentration for overland flow under Green-Ampt Infiltration.” *J Hydrol E – ASCE*, 21(3), doi: 10.1061/(ASCE)HE.1943-5584.0001266, 04015072.

Baiamonte, G., and Singh, V.P. (2016b). “Overland flow times of concentration for hillslopes of complex topography.” *J Irrig Drain E-ASCE*, 142(3), 10.1061/(ASCE)IR.1943-4774.0000984, 04015059.

Broadbridge, P., Daly, E., and Goard, J. (2017). “Exact solutions of the Richards equation with nonlinear plant-root extraction.” *Water Resources Research*, 53:9679–9691, https://doi.org/10.1002/2017WR021097.

Carrión, F., Tarjuelo, J.M., Hernández, D., and Moreno, M.A. (2013). “Design of microirrigation subunit of minimum cost with proper operation.” *Irrig. Sci.*, 31, 1199-1211, 10.1007/s00271-013-0399-8.

De Marchi, G. (1954). *Idraulica*, Hoepli U (ed.). Milan, Italy (in Italian).

Fernández García, I., Montesinos, P., Camacho Poyato, E., Rodríguez Díaz, J.A., 2015. “Energy cost optimization in pressurized irrigation networks.” *Irrigation Sci.*, doi: 10.1007/s00271-015-0475-3.

Gill, P.E., Murray, W., and Wright, M.H. (1989). *Practical optimization*. Academic Press, Inc., San Diego, Calif., 90-91.

Howell, T.A., and Barinas, F.A. (1980). “Pressure losses across trickle irrigation fittings and emitters.” *Trans ASABE*, 23(4): 928–933.

IRRILAB Software application (2018). “Optimal irrigation unit design in one click.” Patent, Ministero dello Sviluppo Economico – Ufficio Italiano Brevetti e Marchi, n° 102015000017479, Nov 3, 2017. https://www.unipa.it/dipartimenti/saaf/ricerca/prodotti.html, http://www.facebook.com/irrilab.

Jiang, S., and Kang, Y. (2010). “Simple Method for the Design of Microirrigation Paired Laterals on Sloped Fields.” *J Irrig Drain E-ASCE*, 136(4), 271–275, 10.1061/(ASCE)IR.1943-4774.0000178.

Jiménez-Bello, M.A., Royuela, A., Manzano, J., García Pratsc, A., and Martínez-Alzamora, F. (2015). “Methodology to improve water and energy use by proper irrigation scheduling in pressurised networks.” *Agric. Water Manag.*, 149:91-101.

Juana, L., Rodriguez-Sinobas, L., and Losada, A. (2002a). “Determining minor head losses in drip irrigation laterals. I: Methodology.” *J Irrig Drain E-ASCE*, 128(6), 376–384.

Juana, L., Rodriguez-Sinobas, L., and Losada, A. (2002b). “Determining Minor Head Losses in Drip Irrigation Laterals. II: Experimental Study and Validation.” *J Irrig Drain E-ASCE*, 128(6), 385-396.

Kang, Y. (2000). “Hydraulic characteristics and computerized design of microirrigation systems.” *Ecosystem Service and Sustainable Watershed Management in North China International Conference*, Beijing, P.R. China, August 23 – 25.

Kang, Y., and Nishiyama, S. (1996). “Analysis and design of microirrigation laterals.” *J. Irrig. Drain. E-ASCE*, 122(2), 75-82.

Kang, Y., Nishiyama, S., and Chen, H. (1996). “Design of microirrigation laterals on nonuniform slopes.” *Irrig. Sci.*, 17:3-14.

Keller, J., and Bliesner, R.D. (1990). *Sprinkle and Trickle Irrigation*, The Blackburn Press, New York, pp: 652. ISBN-13: 978-1930665194.

Palau-Salvador, G., Sanchis, L, González-Altozano, P., and Arviza-Valverde, J. (2006). “Real local losses estimation for on-line emitters using empirical and numerical procedures.” *J Irrig Drain E-ASCE*, 132:6(522), 522-530, 10.1061/(ASCE)0733-9437(2006).

Pitts, D.J., Ferguson, J.A., and Wright, R.E. (1986). “Trickle irrigation lateral design by computer analysis.” Trans. ASAE, 29(5):1320-1324.

Provenzano, G., and Pumo, D. (2004). “Experimental analysis of local pressure losses for microirrigation laterals.” *J. Irrig. Drain. E-ASCE*, 130(4), 318-324.

Rettore Neto, O., de Miranda, J.H., Frizzone, J.A., and Workman, S.R. (2009). “Local head loss of non-coaxial emitters inserted in polyethylene pipe.” *Trans ASABE*, 52(3):729-738.

Sadeghi, S., Peters, R., and Lamm, F. (2015). “Design of zero slope microirrigation laterals: effect of the friction factor variation.” *J Irrig Drain E-ASCE*, 141(10), 10.1061/(ASCE)IR.1943-4774.0000905, 04015012.

Singh, K.G., Goyal, M.R., Rudra R.P. (2015). “Best Management Practices for Drip Irrigated Crops.” Apple Academic Press, Taylor & Francis Group, NY.

Valiantzas, J. D. (1998). “Analytical approach for direct drip lateral hydraulic calculation.” *J Irrig Drain E-ASCE*, 124(6):300-305.

Wang, J., Zhu, D., Zhang, L., and Ames, D.P.J. (2015). “Economic Analysis Approach for Identifying Optimal Microirrigation Uniformity.” *J. Irrig. Drain. E-ASCE*, 141(8), 10.1061/(ASCE)IR.1943-4774.0000863.

Watters, G.Z., and Keller, J. (1978). "Trickle irrigation tubing hydraulics." *ASAE Technical Paper*, 78-2015, American Society of Agricultural Engineers, St. Joseph, MI.

Watters, G.Z., Urbina, J., and Keller, J. (1977). "Trickle irrigation emitter hose characteristics." Proceeding of International Agricultural plastics Congress, San Diego, California, pp. 67-72.

Wu, I.P. (1997). "An assessment of hydraulic design of micro-irrigation systems." *Agric. Water Manag.*, 32, 275-284.

Wu, I.P., and Gitlin, H.M. (1975). "Energy gradient line for drip irrigation laterals." *J. Irrig. and Drain. Div.*, 101(IR4), 321-326.

Wu, I.P., Saruwatari, C.A., and Gitlin, H.M. (1983). "Design of drip irrigation lateral length of uniform slopes." *Irrig. Sci.*, 4(2) 117-135.

Yıldırım, G. (2007). "An assessment of hydraulic design of trickle laterals considering effect of minor losses." *Irrig. Drain.*, 10.1002/ird.303, 399-421.

Yıldırım, G. (2010). "Total energy loss assessment for trickle lateral lines equipped with integrated in-line and on-line emitters." *Irrig. Sci.*, 28:341–352.

Zitterell, D., Frizzone, J.A., and Rettore Neto, O. (2014). "Dimensional analysis approach to estimate local head losses in micro-irrigation connectors." *Irrig. Sci.*, 32:169–179, doi: 10.1007/s00271-013-0424-y.

Notation

c_H [L]	= shifting constant for horizontal laterals
c_S [L]	= shifting constant for sloped laterals
C_v	= manufacturing variation coefficient
D [L]	= internal pipe diameter
D_e [L]	= inner pipe diameter at the emitter section
D_b [L]	= size burb connection of the on-line emitter

EL [-] = equivalent length fraction

EU [-] = emission uniformity coefficient of Keller and Karmeli (1974)

g [L/T^2] = acceleration of gravity

h_i [-] = pressure head at the emitter i

h_{in} [-] = inlet pressure head

h_{min} [L] = minimum allowed pressure head

h_{max} [L] = maximum allowed pressure head

h_n [L] = average (design) emitter's pressure head

$h_{n,L}$ [L] = adjusted nominal (design) emitter's pressure head accounting for minor losses, for sloping laterals

h_{*n} [-] = dimensionless emitter's pressure head

$H(.,.)$ = generalized harmonic number

i [-] = generic emitter of the lateral counted from the manifold connection

i_{min} [-] = number of emitters in a downhill lateral where the minimum pressure head occurs

k_e (L^{3-x} T^{-1}) = coefficient of the flow rate-emitters' pressure head relationship

K (-) = friction loss parameter

K_L (L) = minor loss parameter

K_{*L} (-) = dimensionless minor loss parameter

L_d [L] = length of the lateral by neglecting minor losses

$L_{d,L}$ [L] = length of the lateral by considering minor losses

L_{eq} [L] = equivalent length

m_{EU} = angular coefficient of δ versus EU linear relationships depending on x

$m_{EU,0.5}$ = angular coefficient of δ versus EU linear relationships for $x = 0.5$

n_u [-] = number of emitters in the uphill lateral by considering minor losses

n_d [-] = number of emitters in the downhill lateral by neglecting minor losses

$n_{d,L}$ [-] = number of emitters in the downhill lateral by considering minor losses

n_p [-] = number of emitters per plant

q_{cat} [L^3 T^{-1}] = emitter discharge reported in the catalogue

q_n [L^3 T^{-1}] = nominal emitter discharge

r = flow rate exponent of the flow resistance formula

s = inlet diameter exponent of the flow resistance formula

S [L] = emitter spacing

S_0 [-] = lateral slope

x [-] = exponent of the flow rate-pressure head relationship

x [L] = distance measured from the lateral's inlet

α_L [-] = minor losses coefficient

α [-] = coefficient

α' [-] = coefficient

$(\alpha_L K_{*L}/K)$ = group of variables for horizontal laterals depending on n_d

$(\alpha_L K_{*L}/K)_{10000}$ = group of variables for horizontal laterals for n_d = 10000

$(\alpha_L K_{*L}/S_0)$ = group of variables for sloped laterals depending on n_d

$(\alpha_L K_{*L}/S_0)_{10000}$ = group of variables for sloped laterals for n_d = 10000

γ [-] = shape parameter of the Fréchet EV2 cumulative distribution

δ [-] = pressure head tolerance

δ_e [-] = adjusted pressure head tolerance for sloping laterals

$(\delta h_{*n}/K)$ = group of variables for horizontal laterals depending on n_d

$(\delta h_{*n}/K)_{10000}$ = group of variables for horizontal laterals for n_d = 10000

$(\delta h_{*n}/S_0)$ = group of variables for sloped laterals depending on n_d

$(\delta h_{*n}/S_0)_{10000}$ = group of variables for sloped laterals for n_d = 10000

μ [-] = location parameter of the Fréchet EV2 cumulative distribution

ν [L^2 T^{-1}] = kinematic water viscosity

σ [-] = scale parameter of the Fréchet EV2 cumulative distribution

Table 1 – Examples of calibrated relationships based on empirical data to determine minor losses as a fraction of the kinetic load, α_L, or by the equivalent length method.

Authors	type of emitters	relationship	emitter's sketch
Provenzano and Pumo (2006)	integrated in-line	$\alpha_L = 0.056\left(\left(\frac{D}{D_e}\right)^{17.83} - 1\right)$	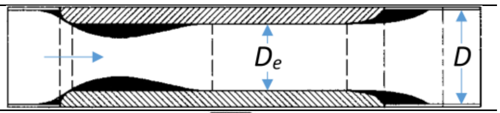
Bagarello et al. (1997)	on-line	$\alpha_L = 1.68\left(\left(\frac{D}{D_e}\right)^{2} - 1\right)^{1.29}$	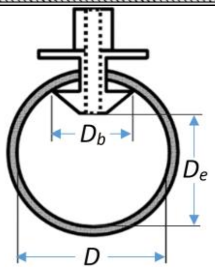
Watters and Keller (1978)	on-line	$l_e = \frac{14.38}{D^{1.89}}$	
Pitts et al. (1986)	on-line	$l_e = 3.5\frac{D_b}{D^{1.86}}$	

Table 2 – Drip lateral characteristics (inside diameter, D, catalogue emitter flow rate, q_{cat}, coefficient, k_e, and exponent, x, of the emitter flow rate–pressure head relationship, emitters' spacing, S), which pertain to TANDEM and JUNIOR® drip laterals, made by IRRITEC, considered in the applications.

Emitter's type	#	D (mm)	q_{cat} (l/h)	k_e	x	emitters' spacing, S (m)
Junior	1	13.6	1.6	0.57	0.46	0.2, 0.3, 0.4, 0.5, 0.6, 0.75, 1, 1.25, 1.5
	2		2.1	0.66	0.5	
	3		3.6	1.13	0.5	
	4	17.6	1.6	0.57	0.46	
Tandem	5	13.6	1.5	0.41	0.57	
	6		2.1	0.69	0.5	

Table 3 – For horizontal laterals, equivalent length fraction, EL, rounded to one decimal place, corresponding to the different parameters, n_d, $\delta h_{*n}/K$ and $\alpha K_{*L}/K$.

EL	**n_d**	$\delta h_{*n}/K$	$\alpha K_{L}{*}/K$	**n_d**	$\delta h_{*n}/K$	$\alpha K_{L}{*}/K$	**n_d**	$\delta h_{*n}/K$	$\alpha K_{L}{*}/K$	**n_d**	$\delta h_{*n}/K$	$\alpha K_{L}{*}/K$	**n_d**	$\delta h_{*n}/K$	$\alpha K_{L}{*}/K$
0.1			0.182			0.157			0.139			0.127			0.118
0.2			0.469			0.405			0.361			0.328			0.306
0.3			0.941			0.819			0.731			0.666			0.622
0.4			1.771			1.555			1.394			1.271			1.188
0.5	15	341	3.362	30	2195	2.990	50	8783	2.694	75	26545	2.464	100	58289	2.307
0.6			6.809			6.172			5.608			5.151			4.833
0.7			15.80			14.78			13.62			12.60			11.87
0.8			47.91			47.55			45.02			42.26			40.11
0.9			271.8			312.7			318.7			311.6			302.2
0.1			0.107			0.100			0.094			0.090			0.084
0.2			0.278			0.259			0.245			0.234			0.218
0.3			0.564			0.526			0.498			0.476			0.443
0.4			1.079			1.006			0.953			0.911			0.849
0.5	150	176953	2.097	200	389448	1.958	250	718385	1.855	300	1184974	1.774	400	2610921	1.654
0.6			4.404			4.115			3.902			3.734			3.483
0.7			10.853			10.162			9.646			9.239			8.624
0.8			36.97			34.75			33.06			31.72			29.67
0.9			284.9			270.9			259.6			250.2			235.4
0.1			0.079			0.072			0.067			0.060			0.056
0.2			0.206			0.187			0.174			0.157			0.146
0.3			0.419			0.379			0.353			0.319			0.297
0.4			0.804			0.727			0.677			0.612			0.569
0.5	500	4819458	1.565	750	14684243	1.416	1000	32376823	1.319	1500	98692982	1.192	2000	217654834	1.110
0.6			3.298			2.985			2.780			2.514			2.341
0.7			8.171			7.402			6.897			6.240			5.811
0.8			28.14			25.53			23.81			21.56			20.09
0.9			224.1			204.4			191.0			173.4			161.7

Table 4 – Minimum and maximum values assumed for the design variables and corresponding dimensionless groups.

variable	MIN	MAX
D_L (mm)	9	32
q_n (l/h)	1	50
K	3.30E-08	0.013
S (m)	0.2	3
K_{*L}	2.03E-09	0.012
δ	0.05	0.2
α_L	0	1
EL	0	0.99
h_n	3	50
h_{*n}	1	250
δh_{*n}	0.05	50
$\delta h_{*n}/K$	3.89	1.52E+09
$\alpha K_{*L}/K$	0	3.68E+05
S_0 (-)	0.005	0.4
$\delta h_{*n}/S_0$	0.125	10000
K/S_0	8.25E-08	2.57
$\alpha K_{*L}/S_0$	0	2.43

Table 5 – For horizontal and sloped laterals, parameters, γ, σ and μ, of the Fréchet (EV2) distribution and the corresponding sum squares error, SSE, and standard error of the estimate, SEE.

lateral	γ	σ	μ	**SSE**	**SEE**
horizontal	0.404	0.311	-0.002	0.005255	0.002706
	0.401	0.307	0.000	0.005453	0.002914
sloped	0.529	$4.260 \cdot 10^{-8}$	$-0.216 \cdot 10^{-8}$	0.001132	0.002385

Table 6 – Values of m_{EU} coefficient of Eqs. (28), for the layouts considered in Baiamonte (2018a) (downhill, horizontal and uphill), and for different values of the exponent x of the emitter q_n vs h_n relationship.

x	**m_{EU}**		
	downhill laterals	horizontal laterals	uphill laterals
0.1	12.45	17.47	10.16
0.2	6.25	8.76	5.11
0.3	4.18	5.86	3.42
0.4	3.15	4.41	2.58
0.5	**2.53**	**3.53**	**2.07**
0.6	2.12	2.95	1.74
0.7	1.82	2.54	1.50
0.8	1.60	2.23	1.31
0.9	1.43	1.99	1.17
1	1.29	1.79	1.06

Note: Bold values refer to x = 0.5 considered in Baiamonte (2018a, Fig. 9b).

Table 7 – For horizontal laterals, parameters' values corresponding to the number of the application indicated in the first column. Bold and underlined values refer to applications repeated, by varying n_d, in the last two lines

#	n_d	L_d (m)	δ	$q_n(q_{cat})$ (l/h)	K	$\delta h_{*n}/K$	h_n (m)	K_{L*}	$\alpha K_{L*}/K$	$(\alpha K_{L*}/K)_{10000}$	EL	$n_{d,L}$	$L_{d,L}$	EU
1	300	225.0	0.1	1.60	4.37E-06	1194982	**<u>39.20</u>**	6.36E-07	5.82E-02	2.46E-02	0.068	280	209.8	0.974
2	250	50.0	0.1	2.10	7.04E-06	723790	10.19	4.11E-06	2.34E-01	9.45E-02	0.201	200	39.9	0.972
3	200	100.0	0.1	3.60	1.81E-05	391841	35.42	4.83E-06	8.02E-02	3.07E-02	0.084	183	91.6	0.972
4	500	100.0	0.1	1.60	1.29E-06	4869061	12.52	8.51E-07	3.31E-01	1.59E-01	0.271	364	72.9	0.974
5	1000	500.0	0.1	1.50	3.91E-06	32755011	**<u>639.8</u>**	8.39E-07	1.72E-01	9.75E-02	0.205	795	397.4	0.968
6	250	125.0	0.1	2.10	7.04E-06	723790	25.47	1.64E-06	9.34E-02	3.78E-02	0.101	225	112.4	0.972
1bis	230	172.5	0.1	1.60	4.37E-06	575479	18.88	6.36E-07	5.82E-02	2.31E-02	0.063	215	161.6	0.974
5bis	200	100.0	0.1	1.50	3.91E-06	391841	7.65	8.39E-07	1.72E-01	6.58E-02	0.158	168	84.2	0.968

Table 8 – For sloped laterals, parameters' values corresponding to the number of the application indicated in the first column. Bold and underlined values refer to applications repeated, by varying n_d, in the last two lines.

#	S (m)	S_0 (-)	n_d	L_d (m)	q_n (l/h)	$\alpha K_{L^*}/S_0$	$\alpha K_{L^*}/S_0$ 10000	EL	$n_{d,L}$	$L_{d,L}$ (m)	δ	$h_{n,L}$ (m)	EU
1	0.75	0.05	300	225.0	1.98	7.77E-06	7.24E-09	0.11	268	200.7	0.120	14.9	0.96
2	0.20	0.10	300	60.0	2.94	3.22E-05	3.00E-08	0.31	206	41.2	0.037	19.8	0.99
3	0.50	0.15	200	100.0	5.55	2.30E-05	9.59E-09	0.14	172	86.2	0.096	24.2	0.96
4	0.20	0.15	500	100.0	4.47	2.22E-05	5.69E-08	0.43	284	56.9	0.017	**<u>88.1</u>**	0.99
5	0.50	0.07	1000	500.0	0.72	2.20E-06	2.24E-08	0.26	738	369.0	1.728	2.7	**<u>0.23</u>**
6	0.50	0.10	250	125.0	3.52	1.85E-05	1.20E-08	0.17	208	104.1	0.071	26.1	0.97
4bis	0.20	0.15	900	180.0	2.49	6.84E-06	5.64E-08	0.43	513	102.7	0.112	24.6	0.96
5bis	0.50	0.07	350	175.0	2.05	1.80E-05	2.27E-08	0.26	257	128.7	0.096	17	0.96

Table 9 – For sloped laterals, relative error (RE) of the maximum and minimum allowable pressure heads, of the i_{min}, and of the emission uniformity coefficient, EU, calculated by using the suggested procedure, with respect to those calculated according to the SBS procedure, for each number of the application reported in the first column.

#	$h_{n,L}$* $(1+\delta)$	h_{max} (m)	RE (%)	$h_{n,L}$* $(1-\delta)$	h_{min} (m)	RE (%)	i_{min}	i_{min} (Eq. 21)	RE (%)	EU	EU (Eq. 27)	RE (%)
1	16.73	16.66	0.00	13.13	13.05	-0.01	118	117	-0.01	0.94	0.96	0.01
2	20.55	20.67	0.01	19.07	19.13	0.00	87	90	0.03	0.98	0.99	0.00
3	26.48	26.53	0.00	21.85	21.86	0.00	75	75	0.00	0.95	0.96	0.01
4	89.67	89.97	0.00	86.62	86.74	0.00	119	124	0.04	0.99	0.99	0.00
5	7.30	7.69	0.05	-1.95	-1.88	-0.04	316	322	0.02	-	0.23	-
6	27.96	27.36	-0.02	24.23	23.69	-0.02	94	91	-0.03	0.96	0.97	0.01
4bis	27.32	27.76	0.02	21.80	21.93	0.01	216	224	0.04	0.95	0.96	0.01
5bis	18.50	18.71	0.01	15.27	15.37	0.01	110	112	0.02	0.94	0.96	0.01

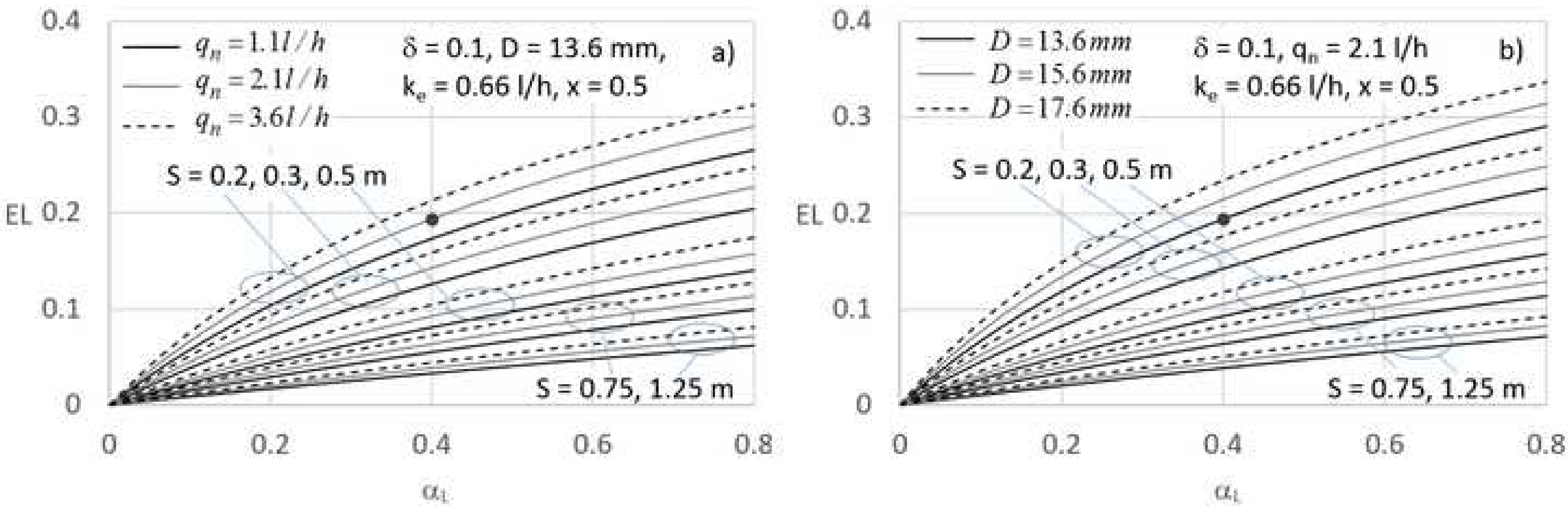

0.4
0.3
0.2
0.1
0
EL
$q_n = 1.1 l/h$
$q_n = 2.1 l/h$
$q_n = 3.6 l/h$
δ = 0.1, D = 13.6 mm,
k_e = 0.66 l/h, x = 0.5
a)
S = 0.2, 0.3, 0.5 m
S = 0.75, 1.25 m
0
0.2
0.4
0.6
0.8
α_L
$D = 13.6 mm$
$D = 15.6 mm$
$D = 17.6 mm$
δ = 0.1, q_n = 2.1 l/h
k_e = 0.66 l/h, x = 0.5
b)
S = 0.2, 0.3, 0.5 m
S = 0.75, 1.25 m

Figure_2

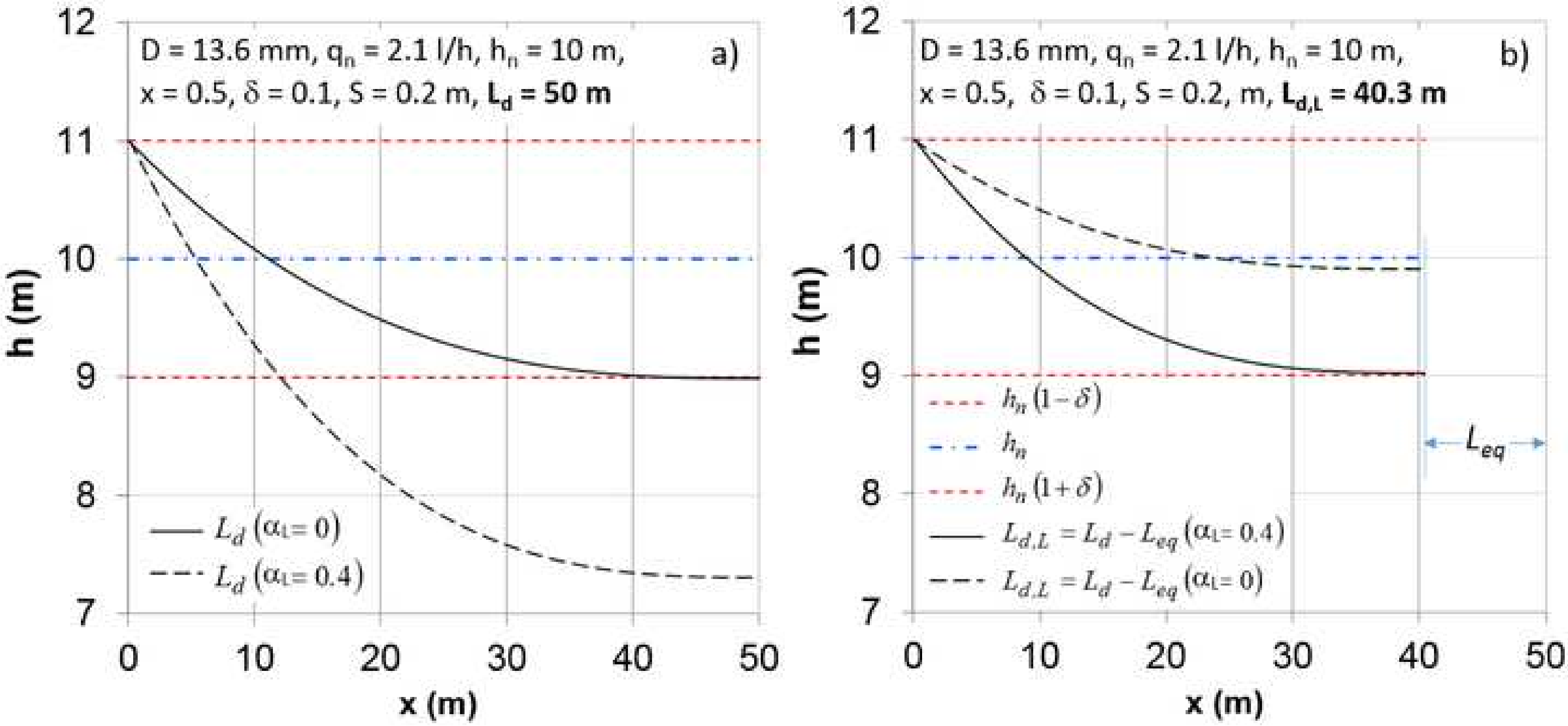

D = 13.6 mm, qn = 2.1 l/h, hn = 10 m,
x = 0.5, δ = 0.1, S = 0.2 m, Ld = 50 m
a)
h (m)
x (m)
Ld (αL= 0)
Ld (αL= 0.4)
D = 13.6 mm, qn = 2.1 l/h, hn = 10 m,
x = 0.5, δ = 0.1, S = 0.2, m, Ld,L = 40.3 m
b)
hn (1−δ)
hn
hn (1+δ)
Ld,L = Ld − Leq (αL= 0.4)
Ld,L = Ld − Leq (αL= 0)
Leq

Figure_3

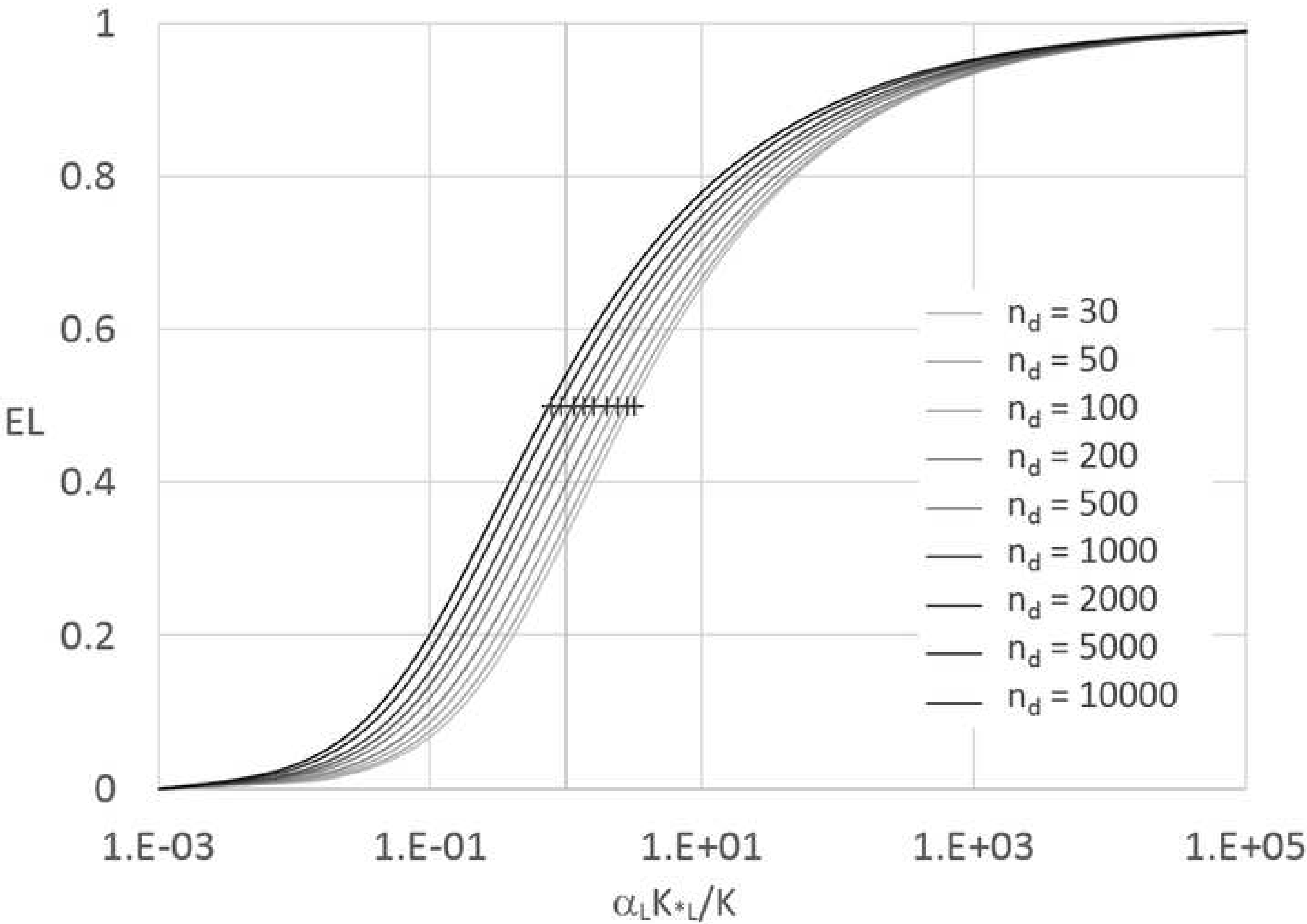

1
0.8
0.6
0.4
0.2
0
EL
1.E-03
1.E-01
1.E+01
1.E+03
1.E+05
$\alpha_L K_{*L}/K$
n_d = 30
n_d = 50
n_d = 100
n_d = 200
n_d = 500
n_d = 1000
n_d = 2000
n_d = 5000
n_d = 10000

Figure_4 Click here to access/download;Figure;Figure_4.tif

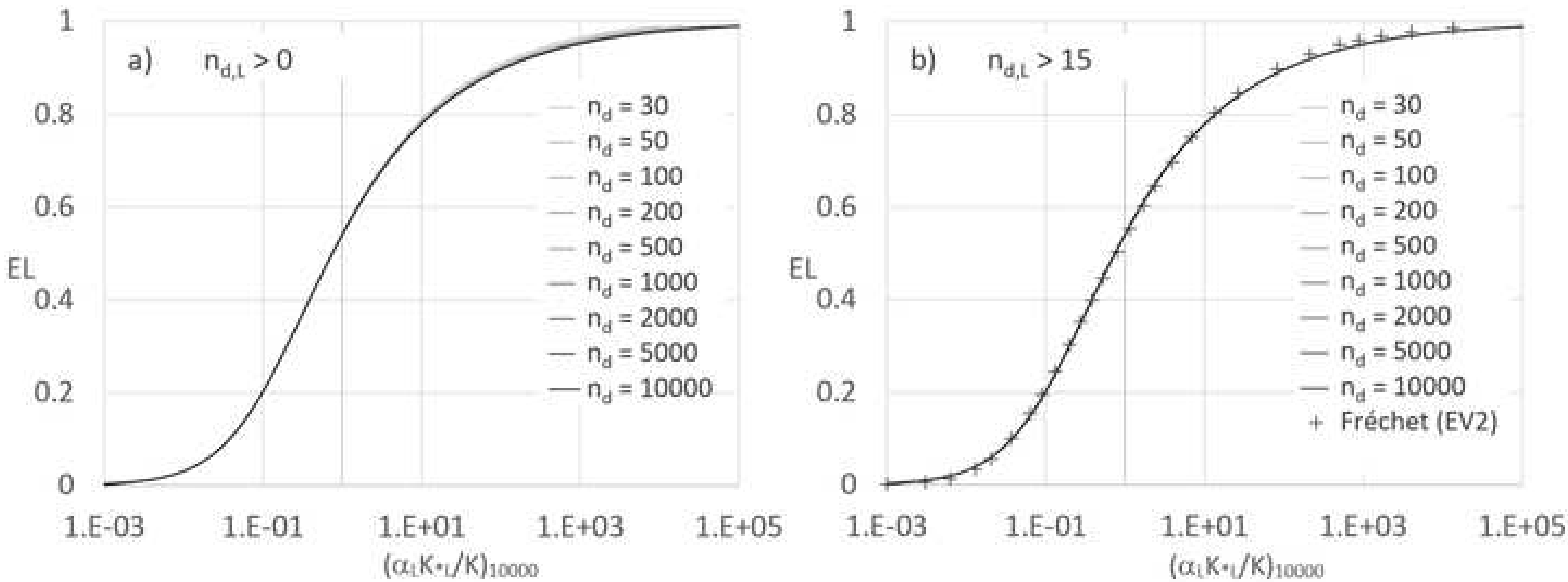

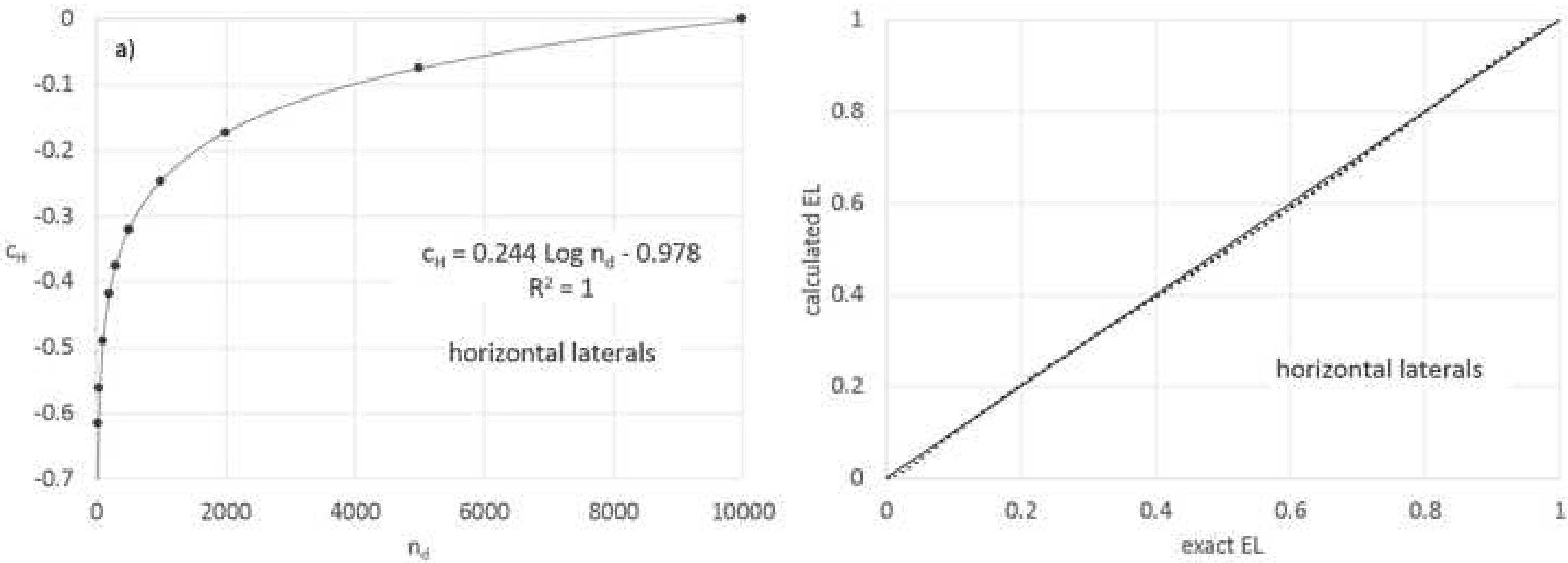
a)
c_H = 0.244 Log n_d - 0.978
R^2 = 1
horizontal laterals
c_H
n_d
0
-0.1
-0.2
-0.3
-0.4
-0.5
-0.6
-0.7
0
2000
4000
6000
8000
10000
calculated EL
exact EL
horizontal laterals
0
0.2
0.4
0.6
0.8
1

Figure_6

Click here to access/download;Figure;Figure_6.tif

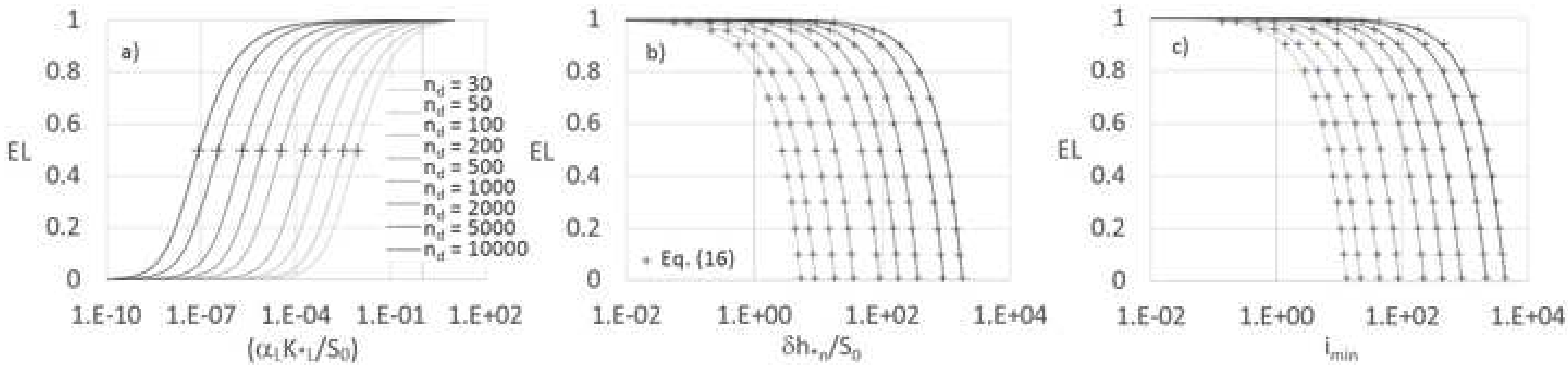

Figure_7 Click here to access/download;Figure;Figure_7.tif

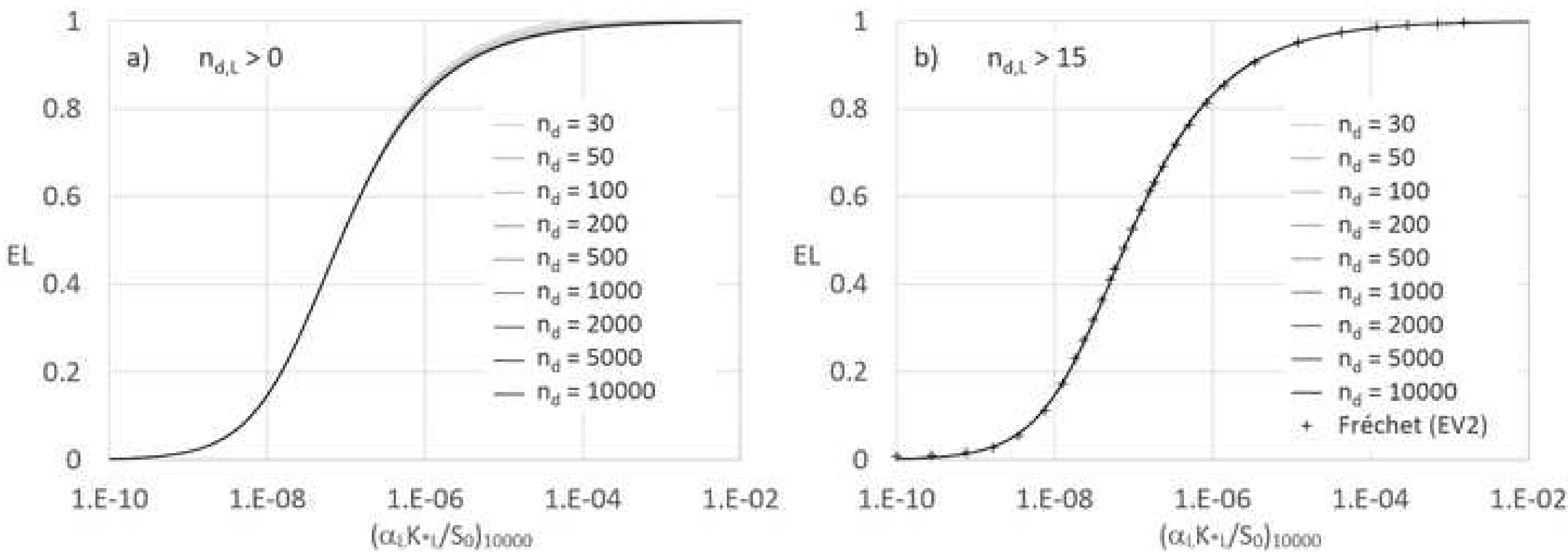

Figure_8

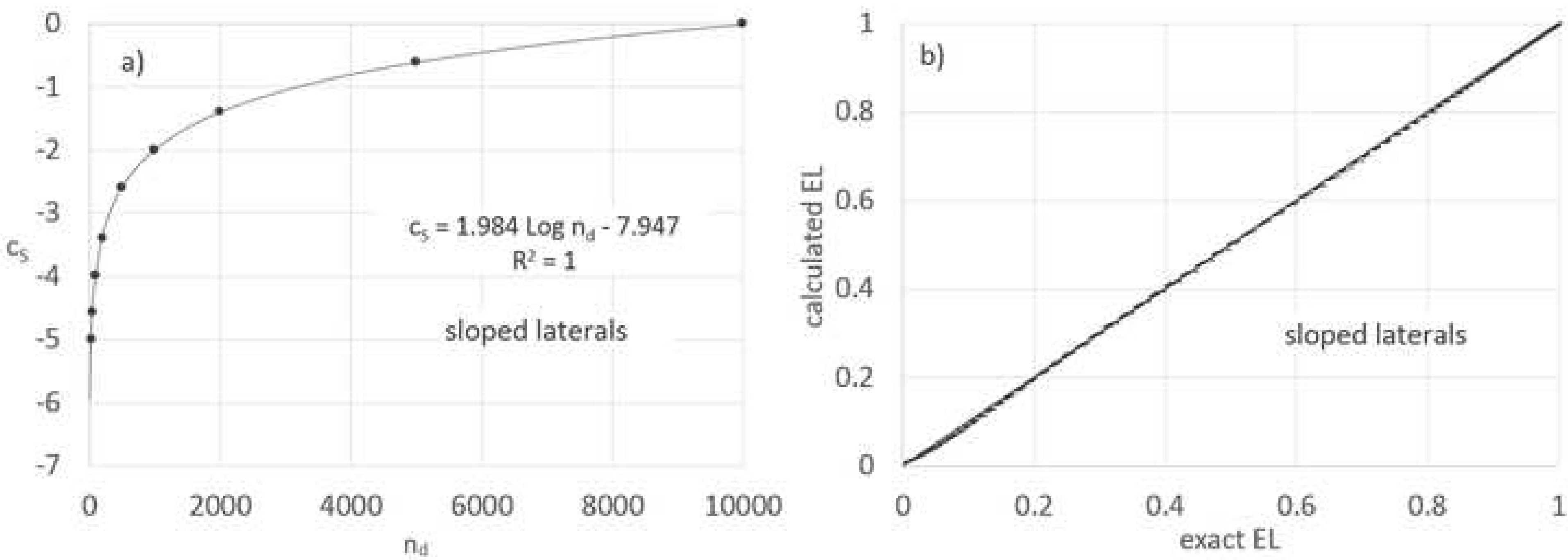

a)
0
-1
-2
-3
-4
-5
-6
-7
c_S
c_S = 1.984 Log n_d - 7.947
R^2 = 1
sloped laterals
0
2000
4000
6000
8000
10000
n_d
b)
1
0.8
0.6
0.4
0.2
0
calculated EL
sloped laterals
0
0.2
0.4
0.6
0.8
1
exact EL

Figure_9

Click here to access/download;Figure;Figure_9.tif

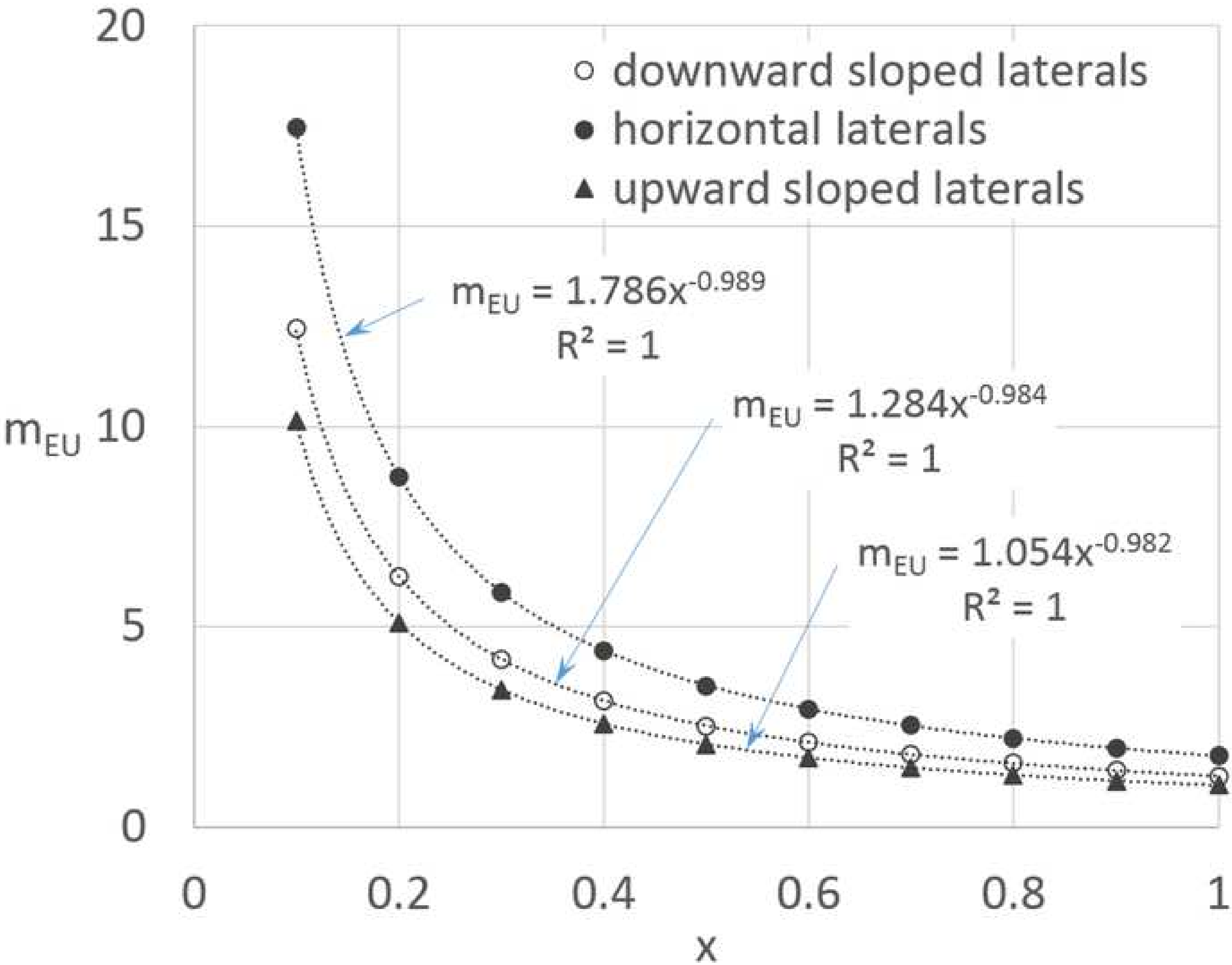

Figure_10

Click here to access/download;Figure;Figure_10.tif

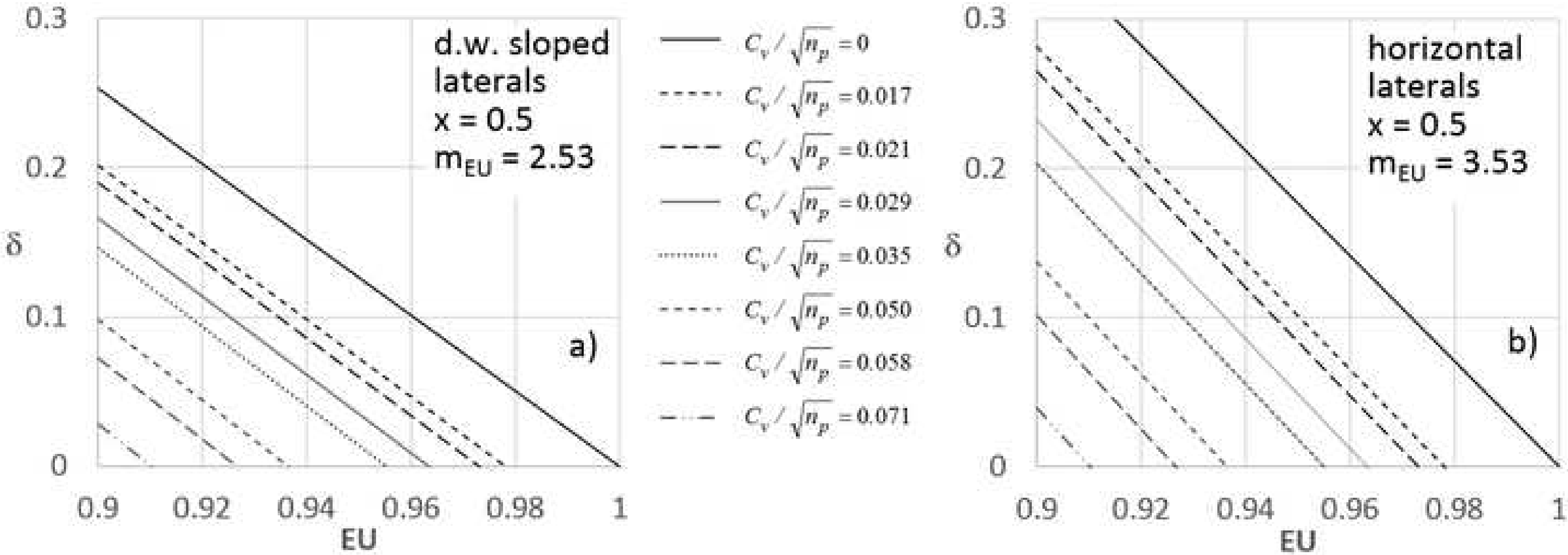

Figure_11

Click here to access/download;Figure;Figure_11.tif

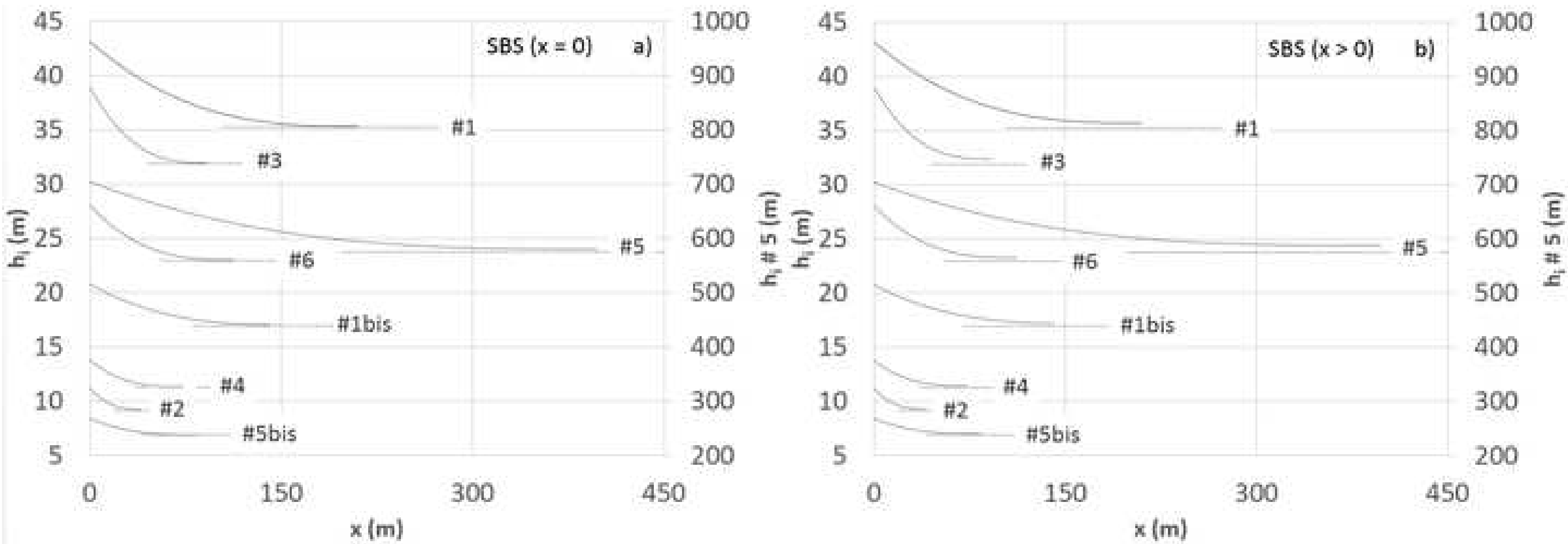

Figure_12

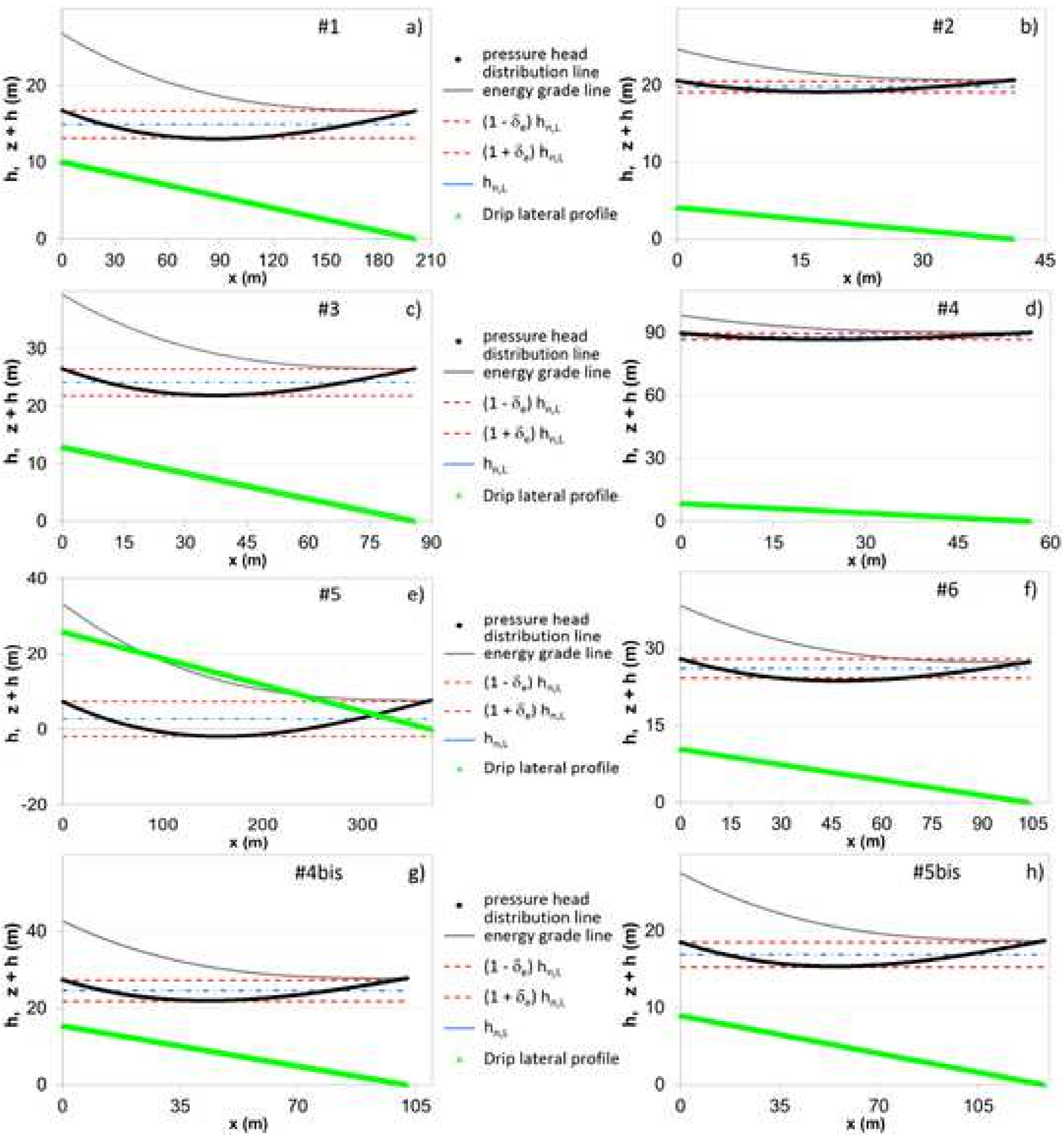

#1 a)
#2 b)
#3 c)
#4 d)
#5 e)
#6 f)
#4bis g)
#5bis h)
pressure head distribution line
energy grade line
(1 - δ_e) h_n,L
(1 + δ_e) h_n,L
h_n,L
Drip lateral profile
h, z + h (m)
x (m)

FIGURE CAPTIONS

Fig. 1 – For horizontal laterals and for different emitter spacing, S, relationship between the equivalent length fraction, *EL*, and the minor losses coefficient, α_L, corresponding to the indicated design parameters values a) for fixed D = 13.6 mm and for different q_n values and b) for fixed q_n = 2.1 l/h and for different D values. Black dots correspond to the example application.

Fig. 2 – For horizontal laterals, a) for $\alpha_L = 0$ and b) for $\alpha_L = 0.4$, and for the other parameters indicated in the text boxes, pressure head lines derived by applying the SBS procedure and by assuming in both cases $\alpha_L = 0$ and $\alpha_L = 0.4$ (see the legend). To $\alpha_L = 0.4$ and *EL* = 0.2 (L_{eq} = 9.7 m, Figure 1b) correspond the black dots illustrated in Figure 1.

Fig. 3 – Relationship between the equivalent length fraction, *EL*, and $\alpha_L K_{*L}/K$, for different n_d (i.e. $\delta h_{*n}/K$). Cross symbols are the median $\alpha_L K_{*L}/K$ values, $(\alpha_L K_{*L}/K)^{median}$, calculated by Eq. (16).

Fig. 4 – For horizontal laterals with different n_d values, equivalent length fraction, *EL*, versus $(\alpha_L K_{*L}/K)_{10000}$ parameter a) for $n_{d,L} > 0$ and b) for $n_{d,L} > 15$. Figure 4b also shows the corresponding *EL* obtained by using the Fréchet (EV2) distribution (Eq. 13, cross symbols).

Fig. 5 – a) Relationship between c_H parameter and n_d (Eq. 12) and b) comparison between the exact *EL* with that calculated according to the Fréchet (EV2) distribution (Eq. 13), with c_H calculated according to Eq. (12) (Figure 5a).

Fig. 6 – For sloped laterals with different n_d values, equivalent length fraction, *EL*, a) versus $\alpha_L K_{*L}/S_0$ parameter, b) versus $\delta h_{*n}/S_0$ parameter and c) for the emitter where the minimum pressure head

occurs, i_{min}. Figure 7b and Figure 7c also show the corresponding *EL* obtained by using Eq. (20). Crosses in Figure 7a are the median $\alpha_L K_{*L}/S_0$ values, $(\alpha_L K_{*L}/S_0)^{median}$, calculated by Eq. (26).

Fig. 7 – For sloped laterals with different n_d values, equivalent length fraction, *EL*, versus $(\alpha_L K_{*L}/S_0)_{10000}$ parameter a) for $n_{d,L} > 0$ and b) for $n_{d,L} > 15$. Figure 4b also shows the corresponding EL obtained by using the Fréchet (EV2) distribution (Eq. 24, cross symbols).

Fig. 8 – a) Relationship between c_S parameter and n_d (Eq. 23) and b) comparison between exact *EL* with that calculated according to the Fréchet (EV2) distribution (Eq. 24), with c_S calculated according to Eq. (23) (Figure 9a).

Fig. 9 – Relationship between the m_{EU} coefficient of Eq. (28) as a function of the exponent *x* of the emitter flow rate-pressure head relationship, for downward, upward and horizontal drip laterals.

Fig. 10 – For different $C_v\ n_p^{-0.5}$ and for $x = 0.5$, pressure head tolerance, δ, as a function of the emission uniformity of Keller and Karmeli (1974), *EU*, a) for downhill laterals and b) for horizontal laterals, according to Eq. (27).

Fig. 11 – For horizontal laterals and for the design parameters reported in Table 7, PHD lines by applying the SBS procedure a) by assuming the exponent $x = 0$ and b) by assuming $x > 0$. Dotted horizontal lines refer to the theoretical minimum pressure value $h_n\,(1-\delta)$.

Fig. 12 – For sloped laterals, application of the suggested procedure for the selected parameters reported in Table 8.